Utilisation of the Geared Five-Bar Slider-Crank Mechanism for Positive Displacement Machines

Azfar Kalim

This Thesis is submitted in total fulfilment
of the requirements for a Masters by Research Degree

School of Science and Engineering

University of Ballarat
PO Box 663, University Drive, Mount Helen
Ballarat, Victoria, 3353
Australia

DECLARATION

Except where explicit reference is made in the text of this thesis, this thesis contains no material published elsewhere or extracted in whole or in part from a thesis by which I have qualified for or been awarded another degree or diploma. No person's work has been relied upon or used without due acknowledgement in the main text and bibliography of the thesis

_____

Azfar Kalim

ACKNOWLEDGEMENTS

I am grateful to my principal supervisor Associate Professor Ibrahim A. Sultan for his outstanding guidance and support during my stay at the University of Ballarat. Thanks are also due to all the staff and fellow students of the School of Science and Engineering.

Abstract

The conventional slider-crank mechanism which is often employed to drive reciprocating positive displacement machines is not adequate when it is necessary to produce non-uniform reciprocations in order to improve machine performance. Instead, this thesis discusses the utilisation of the geared five-bar slider-crank mechanism to drive these machines. This geared mechanism is able to produce favourable stroke characteristics which will not only improve the thermodynamic performance of the positive displacement machine, but will also reduce maximum crankshaft torque and flywheel size. This is expected to increase the service life of machine components and reduce unfavourable dynamic effects.

Whilst Chapter 1 offers introductory discussions and literature survey, Chapter 2 discusses the kinematics of a reciprocating mechanism based on the five-bar geared design. The limiting conditions on the mechanism motion are formulated in terms of a Jacobean matrix, whose determinant is used for the analysis. Insights into the kinematics of the mechanism revealed a new classification based on the nature of the last gear motion.

The focus in Chapter 3 is the design process of the geared five-bar slider-crank mechanism. In this chapter, an optimisation-based ‘dimensional synthesis’ is carried out to calculate the lengths of various links which ensure that the piston will pass via a set of ‘precision’ points during the periodic motion of the mechanism. Synthetic

multi-section curves are employed to guide the motion of the piston but point-to-point matching is not required except at stroke-ends and dwells which are regarded as precision points. At these points, both the position and velocity values obtainable by the designed mechanism are expected to match the corresponding values given by the synthetic curve. The proposed synthesis model features gradient-based Marquardt-Levenberg formulations providing handles that control numerical stability. Numerical case studies are presented at the end of the chapter with results graphed and scaled renderings of the obtained drives drawn.

Chapter 4 presents a compressor case study. The basic premise in the chapter is that the geared five-bar slider-crank mechanism may be dimensioned in such a manner that the kinematic particulars of the resulting stroke may result in optimised performance of a positive displacement machine. This is a two-level optimisation problem: 1. what are the optimum kinematic particulars of the stroke and 2. what are the mechanism dimensions which realize these particulars? To answer these two questions the gradient-based synthesis model presented in Chapter 3 is coupled to a simplified differential thermodynamic model to obtain a drive which optimises a set of selected performance indices for the compressor. A loss function designed to maximise these performance indices is employed in an optimisation procedure based on the approach of Simultaneous Perturbation Stochastic Approximation (SPSA). The stochastic optimisation algorithm employs the particulars of the piston trajectory as the design parameters whilst the stroke length and the bore diameters are kept constant during the optimisation procedure. The results of a numerical example are presented and discussed at the end of the chapter.

Chapter 5 presents some conclusions drawn from the achieved research work and offers insights into possible future endeavours into this field of study.

CONTENTS

LIST OF FIGURES

ABBREVIATIONS

Bottom Dead Centre	BDC
Cyclic Angular Deviation	CAD
Genetic Algorithm	GA
Large Eddy Simulation	LES
Simultaneous Perturbation Stochastic Approximation	SPSA
Structural Analysis Algorithm	SAM
Tabu Search	TS
Top Dead Centre	TDC
United States	US

NOMENCLATURE

ω =	absolute angular velocity
v =	absolute velocity
γ =	adiabatic exponent
θ, μ, φ =	angular displacements of crank
A_{cy} =	bore area
W =	calculated power
V_c =	confined volume of air
C_d =	constant discharge volume
δ =	gear rotations per cycle
ε_r =	critical pressure ratio
A =	cross sectional area
L =	cyclical motion division
V_{cl} =	cylinder clearance volume
V_{cl} =	cylinder clearance volume
C =	Damper coefficient
V =	design vector correction
W =	diagonal matrix
D =	diameter
D =	diameter of gear
C_d =	discharge coefficient
l_a =	distance between first and last gear
η =	efficiency
H =	enthalpy
e =	error expression
U =	fluid velocity
C =	gear centre
β =	gear ratio
Q =	heat produced during cycle
I =	identity matrix
δ =	increment / deflection
J =	kinematic Jacobian
f_p =	loss function
M =	mass
m, ρ =	mass and density of fluid
m =	mass of fluid
$N_{\max}$ =	maximum number of allowable iterations
x =	piston x-coordinate
h =	piston y-coordinate
P =	pressure
g =	quality constraint function

r =	radius of gear
a_i, c_i =	sequence gains
a =	slack variable
J =	system Jacobian
T =	temperature
τ =	torque
R =	universal gas constant
L_v =	valve lift
K =	stiffness
Z_v =	valve motion

Chapter 1

Introduction

1.1 Problem Statement

Reciprocating positive displacement machines are usually driven by a piston-cylinder arrangement attached to a crankshaft by means of a connecting rod. The linear motion of the piston creates pressure variation in the cylinder and is mechanically constrained by the angular displacement of the crankshaft. In order to improve the efficiency of these machines at varying loads and speeds, the drive mechanisms have gone through vast analytical and allied experimentations. As a result, new mechanism designs have been developed with variable stroke lengths and compression ratios necessary to produce non-uniform output reciprocations with uniform rotational inputs. One such design is the geared five-bar slider-crank mechanism, which is the focus of this thesis. The version of this mechanism in which the end gears are pivoted to the frame has been studied by researchers and designers. However, attention was not given to the embodiment in which one of the end gears is pivoted to a slider. This thesis presents design-orientated kinematical insights and mathematical treatments for this embodiment of the mechanism which can be utilised to drive a piston in a piston-cylinder arrangement. This was described in a US patent (US 6,273,052 B1) issued in 2001 to the late Australian inventor Claude Bresland.

The design process of mechanical linkages conventionally features two main activities. First, a ‘type synthesis’ is undertaken to select the type and number of

joints and links used for the mechanism. Then ‘dimension synthesis’ is carried out to calculate the lengths of various links used ensuring that a point on the output link will pass via a set of ‘precision’ points during the periodic motion of the mechanism. For a small number of precision points, closed-form mathematical analysis can be conducted to find the main dimensions of the mechanism. However, the introduction of the computers made it possible to utilise computational-based optimisation techniques in the field of mechanism synthesis. Instead of specifying a small number of precision points to obtain a simplified closed-form solution for the mechanism dimensions, it is now possible to specify a curve on which many points (and even velocities) are defined. Some precision points may be given higher weighting to ensure a better tracing performance for these points.

Despite the advantage offered by the optimisation techniques, they can exhibit numerical instabilities due to the lockup possibilities of kinematic chains. This is more so for gradient-based optimisation techniques. Numerical instability motivated the utilisation of search-based methods in the field of mechanism synthesis. Examples of these methods are the Tabu search (Smaili et al 2005) and the Genetic Algorithms (Liu and Mcphee 2005).

In fact designing a mechanism to drive a positive displacement machine requires an understanding of the thermodynamic aspects of these machines. This will make it possible to design the piston trajectory in such a manner which will ensure more efficient operations. An insight needs to be followed by a synthesis procedure undertaken to obtain an optimised set of mechanism dimensions.

The next section is intended to offer a survey of relevant literature in the area of mechanism synthesis and positive displacement compressors.

1.2 Literature Survey

Etman et al (1998) describe multibody system optimum design problem by design variables, an objective function and constraints. The design variables arise from the bodies, joints and force elements that are present in the multibody system. The objective function and constraints, as they believe, are usually determined by the transient responses following from the numerical multibody analysis. They proposed to couple multibody analysis and optimisation algorithm by approximation concepts.

Liu and McPhee (2005) have based their optimisation framework on a genetic algorithm (GA) for automated type synthesis of planar mechanisms and multibody systems. They believe that the optimisation based approach allows a designer to explore an area for which heuristics are impossible to establish. They also believe that the combination of the GA with a multibody analysis package would allow their approach to generate mechanism designs that closely match the desired kinematic characteristics.

Teng and Angeles (2005), instead of considering the machine elements subjected to loads as a function of time, have followed a novel approach to cope with loads whose magnitudes vary within given bounds and variable directions. The criterion proposed by them is based on condensed normalized stiffness matrix of discretized structure. The boundary of the ellipsoid defined all possible deformations of the structure subject to the same load magnitude in arbitrary directions. They also proposed an arbitrary criterion for maximum stiffness and a given amount of material when the

structure is subjected to variable loading conditions. The criterion, in their view, characterizes the optimum structure pertaining to minimum compliance subject to isometry condition.

Feng et al (2002) have studied planar linkages with clearance at joints and came up with a new optimisation method for their dynamic design taking mass, the centre of mass and the moment of inertia of the moving links as the optimising variables. The changes of amplitude and direction of the joint forces are taken as the objective functions. It revealed that the joint forces were determined by the mass distribution of the moving links when the dimensions of the linkage and input speed were given.

Buskiewicz (2006) presented a method of optimisation by solving a kinematic problem with the use of structural analysis algorithm (SAM) of planar mechanism. His kinematic analysis is based on standard equations in terms of velocities and accelerations. Kinematic problems are expressed in matrix equation form. His structural analysis enables minimizing the expense of numerical solution to the kinematic task, without the use of the methods of mathematical algebra but making use of only topological properties of mechanism.

Sancibrain et al (2004) proposed gradient-based optimisation of path synthesis problems in planar mechanisms by developing a specific formulation to obtain the exact elements of the gradients. They determined sensitivity parameters of all the design variables giving first order relationship between them later using it to enhance the optimisation rate. They have claimed the method to handle equality and in-equality constraints as well as the mobility conditions.

Lio et al (2000) dealt with the use of natural coordinates in optimal synthesis of mechanisms. Like any other multibody system, it is carried out by means of a system of algebric constraint equations complemented by additional equations describing mechanism requirements. They have obtained optimisation by means of classical non-derivative method but used the initial values of the coordinates as a design space rather than link lengths.

Etman et al (1998) used global and mid-range function approximation for engineering optimisation where the commonly used local approximations are not available or applicable. They have described the response surface method to build global and mid-range approximations of the objective and constraint functions. The analysis results in multiple design points were fitted on a chosen approximation model function by means of regression technique.

Spall (1992) presented multivariate stochastic approximation (SA) using a simultaneous perturbation gradient approximation. The author has characterized the bias in the gradient estimate and the algorithm showed to have (almost) sure convergence property of standard finite difference SA algorithm.

Kothandaraman and Rotea (2005) presented simultaneous-perturbation-stochastic-approximation method to minimize the prediction error while estimating the unknown parameters of parachute models from flight-test data, which is capable of optimising any number of parameters in a reasonable time. This is due to the fact that the number of cost function evaluations needed to estimate the gradient which are independent of the number of parameters to be optimised. The method may handle nonlinear dynamic models, non-equilibrium transient test conditions and data

obtained in closed loop. It, therefore, looks equally suitable for the estimation of parameters in guided parachute models.

Tai et al (2002) demonstrated the synthesis of path generating compliant mechanism by the process of topology and shape design optimisation on a micro electro-mechanical system. This suitability, as they believed, is mainly due to the monolithic nature of compliant mechanism giving advantages like no need for assembly, no friction / wear and hence no need for lubrication and no backlash.

Zhang et al (2000) presented a method for primal-dual interior point for linearly convex nonlinear programming and computational experience in solving optimal design problems using the algorithm. In their view the number of design variables and constraints increased greatly in convex programming problems but the number of iterations for approximate optimal solution increased slightly only. They also show that the solution so obtained was an interior point of the feasible region and that the number of function evaluations was only one more than the number of iterations.

Mundo and Yan (2007) have researched on the kinematic optimisation of ball-screw transmission mechanism proposing a method for the kinematic optimisation where non-circular gears are used to perform mechanical control on the output motion. Their objective remains lowering of the peak acceleration value of the screw, by designing a pair of variable radius gear as a driving mechanism. They derived a non-dimensional equation of motion by kinematic analysis of the mechanism later formulating an optimisation problem to reduce internal loading problems during the working stroke.

Cossalter et al (1992) have presented their study on numerical method for optimum synthesis of planar mechanisms, generators of functions, paths and rigid motions. In their view, the design parameters have wide variety ranges, inside which first guesses could be chosen at random as demanded by the iterative minimization procedure. They carried out kinematic analysis by decomposition of the mechanism into Assur groups and the mechanism assembly is managed by construction of a proper penalty function. Optimisation was carried out by using a non-derivative and quasi-Newton method in series. They also reported that it performed well especially when two minimization subordinates were used in series.

Dooner (2001) presented a procedure for generating any desired function using an eight-link mechanism incorporating optimised non-circular gear elements. A desired function that relates an arbitrary input parameter to its corresponding output parameter was used to develop equations for the synthesis of a non-circular gear pair and a corresponding mechanism was specified for coordinated steering to illustrate the methodology. Specific automotive parameters were given and corresponding mechanism was specified for coordinated steering. Subsequently, the optimisation of certain mechanism parameters that minimize the non-circularity of the gear pair was presented.

Smaili et al (2005) have employed the Tabu-Search (TS) method augmented with the gradient search to find optimum solution to synthesis problem of a four-bar mechanism. In their view, the Tabu-gradient algorithm was capable of realizing optimal solutions better than those obtained by other optimisation schemes, which

includes the Central Difference, Exact Gradient, Genetic Algorithm with various operators, and Genetic Algorithm coupled with Fuzzy Logic.

Smaili and Diab (2007) introduced a new approach to shape optimisation for closed-path synthesis of planar mechanisms with their two-step method to synthesize four-bar mechanism traversing close trajectories; shape synthesis followed by translation, rotation and scaling synthesis. The objective function is not based on Fourier descriptors, but rather on the cyclic angular deviation (CAD) vector associated with a set of desired points on the curve. They proposed a simple method to determine analogous starting points on the desired and generated curves followed by purely mathematical procedure applied to scale, rotate, and translate the mechanism for the advantage of their method; (i) using lesser variables and (ii) being insensitive to the shape of the coupler curve and to any sharp edges it may have.

Cabrera et al (2002) presented a new method based on an evolutionary technique for path synthesis of planar mechanisms. They introduced an algorithm to optimise the position error between the target points selected by the designer for the couple point and the points reached by the resulting mechanism, subject to different constraints. For their synthesis, they employed four-bar planar mechanism to test their method.

Deb and Tiwari (2005) have studied evolutionary multi-objective optimisation of a leg mechanism using genetic algorithms. A leg mechanism design problem involved link length and spring characteristics as decision variables. The problem provided a number of challenges to any optimisation algorithm such as: multiple objectives, highly constraint search space, highly non-linear objective and constraint function and last but not least a lot of linked decision variables. The authors have approached

the compound leg mechanism problem with spring elements and treated it as a whole providing optimised solution of three different objectives using the evolutionary multi-objective optimisation procedure.

Martin et al (2007) have studied mechanism design for motion generation to select planar four-bar motion generators with respect to Grashof conditions, transmission angle conditions and having the minimal perimeter value. Methods like Brumester curve-based motion generation, in their view, produced an infinite number of solutions for a prescribed series of rigid-body poses. Search and select process is used in order to adhere to specific mechanism design conditions and constraints.

Gatti and Mundo (2007) have studied optional synthesis of six-bar cam-linkages for exact rigid body guidance. They consider two linear and one angular displacement of a six-bar linkage with three degree of freedom, for the designer to specify any number of precision configurations. Using inverse kinematic analysis, the independent parameters are evaluated. They propose to reduce the mobility by synthesising two cam pairs on the basis of the relationships between the linear displacements, but the angular one is kept as independent variable. In their view the resulting mechanism might be able to exactly guide a rigid body through any number of precision configurations.

Minaar et al (2001) presented a method for treating non-assembly in the optimal synthesis of planar mechanisms. They performed synthesis with gradient based optimisation algorithms and sensitivities were calculated analytically through the method of direct differentiations. Their analysis was based on the well-established and general method of computational kinematics. They have minimized the residual

of the joint constraint equations rather than equating it equal to zero. This made it possible to perform the kinematic analysis for any proposed design even though it might not be possible to assemble the mechanism.

Hansen (2002) proposed a method for the synthesis of mechanisms using time-varying dimensions in which the problem is overcome by allowing the dimensions to vary during the motion of the system and subsequently minimizing the deviation of each variable dimension over a cycle. In his method the dimensions for each step are allowed to change in order to obtain assembly as well as a desired kinematic behaviour. This method may handle the non-assembly problems for synthesis of general mechanisms. The dimensions of the system are the design variables and allowing them to vary during the motion of the mechanism might guarantee that the system could be assembled at all configurations. The synthesis problem was then solved by attempting to minimize the deviation of the design variable during a cycle.

Jensen and Hansen (2006) presented a general method of dimensional synthesis of both planar and spatial mechanisms. Their method addressed the problem of non-assembly. They employed a gradient based optimisation algorithm and calculated sensitivities analytically using direct differentiation. To avoid non-assembly problem, they slightly modified a well established general method of computational kinematics. The modification consisted of the minimization of the residuals of kinematic constraint equations, rather than equating them to zero. They applied point-coordinate formulation which describes a mechanism as a collection of interconnected points for example the end points of a body.

Shiakolas et al (2005) have presented the optimum synthesis of six-bar linkages using differential evolution and the geometric centroid of precision positions technique, which they also described as synthesis of six-bar mechanisms with prescribed timing. In their view, six-bar mechanisms are synthesised when a dwell is desired at the output link as a function of input link. They have called their evolutionary algorithm as 'Differential Evolution' which has been used along with a novel technique for variables called 'Geometric Centroid of Precision Points'. Two Penalty functions were also employed in the optimisation process; one emphasizing on the deviation from precision points and second penalizing constraint violation irrespective of magnitude.

Haung and Roth (1993) researched on three planer linkages; four-bar, slider crank and double-slider crank. They combined classical kinematic synthesis to consider force conditions as well as motions in the dimensional synthesis of linkages. Their concern was to determine the dimensions of linkages that guide a rigid body through several positions and support a specified external load at each position. The methodology developed was based on the principles of kinematics and statics. They showed that the principal of virtual work may be used for efficient formulation of the static equation. In planer rigid-body guidance problems, introducing force specifications reduced the maximum number of allowable specified positions. They also showed that additional design positions are obtained from the incompletely specified positions and force problems.

Yu and Lee (1996) have performed curvilinear optimisation of a cam mechanism with a translating flat-faced follower based on flexible motion curves using parametric polynomials to maximize the minimum radius of cam curvature. They

have shown that using their technique brings a control over both the kinematic feature of the motion curve as well as the curvature of the cam profile.

Suchora and Savage (1974a and 1974b) have thoroughly explored geared five-bar crank mechanism with graphical and analytical kinematic analysis as well as presenting a static force analysis and motion classifications. It has been shown that a five-bar chain has 2-degrees of freedom requiring two inputs to obtain a definite controlled output. In such a mechanism constraining any two non-adjacent links makes a five-bar chain to a useful five-bar mechanism producing a large set of output motions, using circular gears. Their work made available practical planar mechanism to the designer for such motions which could not be produced easily by other linkages but form these efficient mechanisms. The types of motion considered in their work are crank rocker and double crank. The desirable motions which may be produced are; (i) rotary oscillations and full cycle rotations with intermediate dwells (ii) full cycle rotations with intermediate oscillations (iii) two or more output rotations and / or rotary oscillations from one input rotation. In their view, the output axis might not be fixed in the frame and thus oscillate radially becoming a major drawback of the mechanism.

Nokelby and Podhorodeski (2001) have developed a Grashof five-bar mechanism synthesis routine, using convergence criteria of (i) objective function value (ii) mechanism parameter change and (iii) task satisfaction. Their developed sequential unconstrained search variable to constrained design parameter transformation set, ensures the synthesis of Grashof geared five-bar mechanisms of a desired sub-type with design parameters between desired upper / lower bounds.

Bresland (2001) presented his invention providing a coupling arrangement for inter-connecting a gudgeon arrangement and a crankshaft journal of a reciprocating piston engine. In this invention the point of attachment of the connecting rod as in conventional engines is separated from the gudgeon pin by a connecting member pivotally attached between the connecting rod and the gudgeon pin. With such an arrangement, it is possible to create a reciprocating piston engine in which the crankshaft journal need no longer be at a top centre position when the piston is at its top dead centre position. The object of the invention was to provide a reciprocating piston engine which overcomes or ameliorates one or more of the disadvantages of known reciprocating piston engines.

Work of Sultan (2002), on five-bar geared mechanism, has important application in the positive displacement machinery. The differential nature of gear kinematics always compounds the difficulty of position analysis performed on these mechanisms. He has developed a mathematical model for kinematic analysis of a new geared-coupled mechanism. The presented model integrates the gear velocity equation into a form, which may be combined with the geometric constrained equations to perform the analysis. It is also shown that, despite their versatility, these mechanisms exhibit mathematical singularity during assembly.

Dagilis et al (2006, 2007a and 2007b) have studied slider-link driven compressor used in household refrigerators. Although these are now considered outdated, yet still in production, with some advantages in their view, when displacement is decreasing. The main disadvantage is high losses for friction in a slider-link pair which was overcome by using connecting rod with spherical joint. Dagilis et al claimed that the mathematical model developed by them is multi-task oriented which possibly could

be useful for the designer to calculate forces and dynamic behaviour of slider-link driven compressor. The model is also useful for compressor optimisation like compressor's geometrical parameters, to ensure its highest efficiency. They continued to claim the validity of their model for the cost effective technological improvements and finally as means to justify translation to slider-driven compressors.

Catto and Prata (2000) presented a numerical analysis of the flow and heat transfer in a gas confined by a moving piston inside a valve-less cylinder showing that the in-cylinder heat transfer was out of phase with the bulk gas-wall temperature difference and the conventional Newton's law did not seem applicable. They also observed that the heat transfer should also depend on the time derivative of the bulk gas temperature. They have modeled the unsteady compressible axisymmetric flow inside the cylinder using a moving coordinate system and a finite volume methodology which explores the existing phase difference between the heat transfer and the gas-wall temperature difference. Their work correlates computational results obtained from the full continuity, momentum and energy equations with empirical expressions, for the first time as claimed by them, bringing it to light that any successful correlation must include the time derivative of the gas temperature. They also stressed that the understanding of the in-cylinder heat transfer is essential in modeling compressors, internal combustion engines, and other reciprocating machines.

Rigola et al (2004) performed a detailed analysis of the thermal and fluid dynamics behaviour of hermetic reciprocating compressor using a household appliance compressor. The fluid and the solid thermal map evolution was logged in several

strategic points. The absolute instantaneous pressure was also measured in three specific zones; (i) suction muffler (ii) compression chamber and (iii) cylinder head. This experimental approach allowed the authors to validate a mathematical model developed for the numerical simulation of the thermal and fluid dynamic behaviour of hermetic reciprocating compressor bringing out that more efforts might be needed on specific details like the heat transfer empirical input used and dynamic model of the inlet and exhaust fluttering valves.

Rovaris and Deschamps (2006) consider the application of large-eddy simulation (LES) to predict the performance of hermetic reciprocating compressors for refrigeration, in which the piston motion establishes the valve opening; after which pressure distribution is dictated by flow and the resultant force governing valve dynamics and their displacement from the seat. The authors adopted one-degree of freedom model for valve dynamics and a finite methodology to solve the flow field throughout the discharge valve. For suction valve an integral formulation was employed with effective flow and force areas being used to evaluate the dynamics and mass flow rate. The solution procedure combined the integral and differential formulations. Important phenomena occurring in the discharge process were observed like backflow through discharge valve and over-shooting cylinder pressure.

Estupinan and Santos (2007) have presented a multibody dynamic model of the main mechanical components of a hermetic reciprocating compressor. The dynamics of the mechanical components are described with the help of dynamics of multibody systems for rigid components and finite element method for flexible components. The system of nonlinear equations is numerically solved, taking into account the lateral and tilting vibrations of the centre of the crank.

Stouffs et al (2001) presented a global model for the thermodynamic analysis of reciprocating compressors. Their model is based on five main and four secondary dimensionless physically meaningful parameters and expressions for volumetric residual mass fraction. The specific work and indicated efficiency were derived. It was made evident that heat transfer during suction from cylinder walls, the valve pressure losses and the work needed to displace the fluid, the heat transfer to fluid during compression and heat transfer to the residual mass during expansion affect the performance of a reciprocating compressor. Their computational and experimental results showed close agreement.

Lekic and kok (2008) have extensively studied heat flows in piston compressors. To improve the design and reliability of compressor designs, they focused on the transient thermal and fluid flow phenomena and thermo-mechanical processes in an unbiased piston-cylinder gas spring. In their view the conditions of fluid were far from the flow situation which was encountered in a piston cylinder gas spring. They described the flow as oscillatory in character, which is almost arrested in top and bottom dead positions and at maximum speed in between. Axial and radial velocity gradients also existed. Axial fluid velocity equals the piston velocity at its surface and vanishes at the cylinder head; the axial motion exciting the radial motion and turbulence. Therefore, they took into account complicated transient and local fluid mechanical and thermodynamic phenomena. They have discussed suitable turbulence models, near wall heat transfer modeling and modeling of fluid flow structures developing in the gas flow above the piston.

Shu et al (1997) incorporated frequency-dependent friction in their distributed parameter to model pressure pulsations in reciprocating pump piping systems. They interfaced it with a pumping dynamics of a plunger pump to allow time-domain simulations of pipeline pressure pulsations in both suction and delivery lines. In their view the current model remained inadequate for the distributed parameter nature of the pipeline and also due to cavitation.

Nieter and Singh (1984) have studied simulation of compressor tuning phenomena and found it to be dependent upon the acoustic behaviour of the manifolds. They discussed the complexity of the problem as increase in mass flow rate did not correspond with higher energy efficiencies. Their simulation model included the manifold back pressure effect, to investigate and explain the tuning phenomena for a positive displacement reciprocating compressor. They presented their results for the flow efficiency, energy efficiency and pressure pulsations at valve exit in terms of acoustic natural frequencies of the manifold system. In their view their study helped choosing optimal manifold dimensions thus providing higher efficiencies with lower pressure pulsations.

Cho and Moon (2005) performed a numerical analysis on the interaction between the piston oil film and component deformation in a reciprocating compressor. In their view, the secondary motion significantly influences the major characteristics of lubrication in a reciprocating compressor, such as the oil leakage, the piston slap phenomena and the frictional power loss. They stressed upon reliable dynamic characteristic investigation upon the design parameters governing piston dynamics. They have treated both piston and cylinder as deformable bodies in the lubricant-structure interaction. The oil flow and the power consumption show ‘time-history’

responses dominated by piston velocity pattern but extreme points seemed to be influenced by axial pressure gradient and also found some structure flexibility giving rise to some effect on the radial clearance change with varying magnitude.

Peng et al (2002) performed thermodynamic analysis of the rotary tooth compressor by constructing a mathematical model to simulate the thermodynamic processes within it to predicting its performance. Loss in capacity is most affected by gas leakage and the main cause of loss in adiabatic efficiency is the power loss associated with high gas velocities during discharge process. Authors believed that over compression at start could be unavoidable which could only be reduced a little by decreasing the rotational speed.

Sultan (2005) has studied limacon of Pascal which is a plane curve suitable for fluid processing applications. The presented work was meant to explore various mechanical linkages that can be employed to produce the limacon and study different aspects of these linkages. The mathematical analysis showed that the machines based on limacon curves possess sinusoidal volumetric relationships and hence, simplified pressure and torque equations could be obtained in closed form. A compressor was taken as a sample application.

Sultan (2006) presented the profiling for limacon-to-limacon compression-expansion machines, which have their housings and rotors profiles manufactured to limacon curves. He suggested that the main characteristics are volumetric efficiency and prevention of interference that govern the quality of rotor profile. He has handled the interference problem from two different mathematical stand points: the slope of tangents to both the rotor and housing curves at the apices, and the value of

minimum radial clearance that separates the two limacon curves. In the first case, mathematical expressions, relating to the radii of limacon base circle are presented to ensure that interference would not take place during normal operations of limacon-to-limacon machine. The second mode of analysis produces a set of nonlinear equations that may be solved to obtain a value of radial clearance. This value has to be machined off the rotor profile to prevent interference. A numerical example of a limacon-to-limacon compressor is given to prove the validity of the models proposed.

1.3 Scope of the Thesis Work

The main theme in this thesis is the utilisation of the geared five-bar slider-crank mechanism to drive positive displacement machines. To introduce the reader to the aspects of this mechanism a kinematic model will be presented and solved numerically. The limiting conditions on the mechanism motion will be formulated in terms of Jacobean matrices whose determinants will be used for the analysis.

A synthesis model will be proposed which will be based in the Marquardt-Levenberg formulation. This formulation does provide handles which can be employed to control the convergence rate and increase numerical stability. During the optimisation procedure, multi-section synthetic curves will be used to guide the motion of the piston but point-to-point matching is not required except at stroke ends and dwells, which are regarded as precision points. At these points, both the position and velocity values obtainable by the designed mechanism are expected to match the corresponding values given by the synthetic curve. Case studies will be presented to demonstrate this synthesis procedure and prove its validity.

To demonstrate how the geared five-bar slider-crank mechanism can be utilised to improve the thermodynamic workings of a positive displacement machine, a reciprocating compressor case study will be presented. A differential thermodynamic model for the compressor will be coupled with the gradient-based synthesis model to obtain a drive which optimises a set of performance indices. For this purpose a hybrid optimisation technique will be formulated to combine the gradient-based synthesis with the stochastic-based simulation. The obtained results will be presented to prove the suitability of the proposed approach for the tackled problem.

It may be added here that the gear-coupled mechanisms are known to have their own advantages such as high efficiency and low maintenance cycles while transmitting large power over short distances. If properly designed, these mechanisms are highly reliable at high speeds with high precise timing and constant speed ratios. On the other hand, they can be noisy at high speeds and produce heat which has to be taken away by a suitable lubricant. Also the inclusion of gears may increase the manufacturing cost of the mechanism. However this may not be a real problem in mass production situations.

Chapter 2

Kinematic Analysis of the Five Bar Slider-Crank Mechanism

2.1 INTRODUCTION

The version of the five-bar geared mechanism in which end links are pivoted has been studies by researchers like Suchora and Savage (1973 a, 1973 b). However these researchers did not give much attention to the embodiment in which one of the end gear is a slider. This specific case is the focus of present thesis due to the remarkable potential it offers to the position displacement applications. In order to improve the overall performance (power and volumetric) of positive displacement machines at varying loads and speeds the reciprocating mechanisms have gone through vast analytical studies and allied experimentations. New mechanism designs have been developed with variable stroke lengths and compression ratios necessary to produce non-uniform output reciprocations with uniform rotational inputs.

In this chapter the kinematics of a reciprocating mechanism based on the five-bar geared design will be studied. Suchora and Savage (1973 a) referred to this

embodiment as the "crank mechanism" and Bresland (2001) later suggested that it can be used to drive a piston in a piston-cylinder arrangement. Four bar chains cannot produce dwells of useful durations which is one of their limitations. When a link is added to a four-bar chain, it increases the variety of output motions, longer dwells and better force transmission. Suchora and Savage (1973 a and 1973 b) point out that five-link chain has two-degrees of freedom requiring two inputs to obtain a definite controlled output. In such a mechanism constraining any two non-adjacent links, using circular gears, transforms the five-bar chain to a useful five-bar mechanism capable of producing a large set of output motions. They also pointed out that gears may be assembled at any initial angles as against linkages which have to be assembled in a specific configuration for given crank angles.

In this chapter a position model is introduced and solved numerically for the five-bar geared slider-crank mechanism. Insights into the kinematics of the mechanism will reveal a new classification based on the nature of the last gear motion. Kinematic Jacobeans are used to determine motion limitations and find the stationary positions of the slider. The next section presents modeling of gear train part of the five bar slider-crank mechanism.

2.2 MODELING OF THE GEAR TRAIN

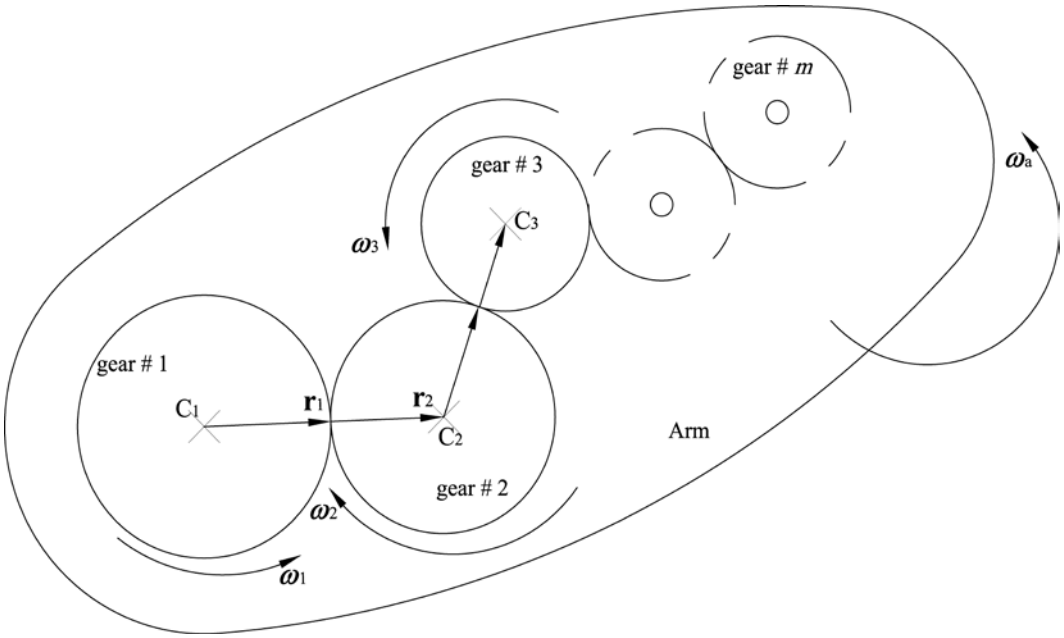

Figure 2.1 The Gear Train Set

Figure 2.1 shows a gear train set with all its gears pivoted to a floating arm. The absolute velocity vectors, $\mathbf{v}_{c1}$ and $\mathbf{v}_{c2}$, of the gear centres, C_1 and C_2 are related as:

$$\mathbf{v}_{c2} - \mathbf{v}_{c1} = \boldsymbol{\omega}_a \times (\mathbf{r}_2 + \mathbf{r}_1) \qquad 2.1$$

where $\boldsymbol{\omega}_a$ is the absolute angular velocity of the arm and the position vectors, $\mathbf{r}_1$ and $\mathbf{r}_2$ define the radii of gear 1 and 2 respectively. The velocities in the above equation 2.1 may be related in the following vector equation:

$$\mathbf{v}_{c2} - \mathbf{v}_{c1} = \boldsymbol{\omega}_2 \times \mathbf{r}_2 + \boldsymbol{\omega}_1 \times \mathbf{r}_1 \qquad 2.2$$

where $\boldsymbol{\omega}_1$ and $\boldsymbol{\omega}_2$ are absolute angular velocity vectors of gear 1 and gear 2 respectively.

Comparing equations 2.1 and 2.2

$$\boldsymbol{\omega}_2 \times \mathbf{r}_2 = \boldsymbol{\omega}_a \times \left(\mathbf{r}_2 + \mathbf{r}_1\right) - \boldsymbol{\omega}_1 \times \mathbf{r}_1 \qquad 2.3$$

Since the vectors $\mathbf{r}_1$ and $\mathbf{r}_2$ are always collinear and $\boldsymbol{\omega}_a$ is parallel to both $\boldsymbol{\omega}_1$ and $\boldsymbol{\omega}_2$, the above equation may be expressed in a scalar form:

$$\omega_2 r_2 = \omega_a \left(r_2 + r_1\right) - \omega_1 r_1 \qquad 2.4$$

where r_1 and r_2 are pitch circle radii of gear 1 and gear 2 respectively.

Similarly the angular velocity, ω_3 of gear number 3 may be expressed as:

$$\omega_3 r_3 = \omega_a \left(r_3 + r_2\right) - \omega_2 r_2 \qquad 2.5$$

where r_3 is pitch circle radius of gear 3.

Equations 2.4 and 2.5 may be combined to obtain ω_3:

$$\omega_3 r_3 = \omega_a \left(r_3 - r_1\right) - \omega_1 r_1 \qquad 2.6$$

Comparison of the Equations 2.4 and 2.6 leads to relating angular velocity ω_m of gear m to the angular velocity of gear 1 and the arm:

$$\omega_m r_m = \omega_a \left(r_m - (-1)^{m-1} r_1\right) + (-1)^{m-1} \omega_1 r_1 \qquad 2.7$$

where r_m is the pitch circle diameter of gear m.

Multiplying equation 2.7 by 2 and dividing throughout by D_m, the diameter of gear m:

$$\omega_m = \omega_a \left[1 - (-1)^{m-1} \left(\frac{D_1}{D_m}\right)\right] - (-1)^{m-1} \omega_1 \left(\frac{D_1}{D_m}\right) \qquad 2.8$$

where D_1 is the pitch circle diameter of gear 1.

2.3 KINEMATIC EQUATIONS

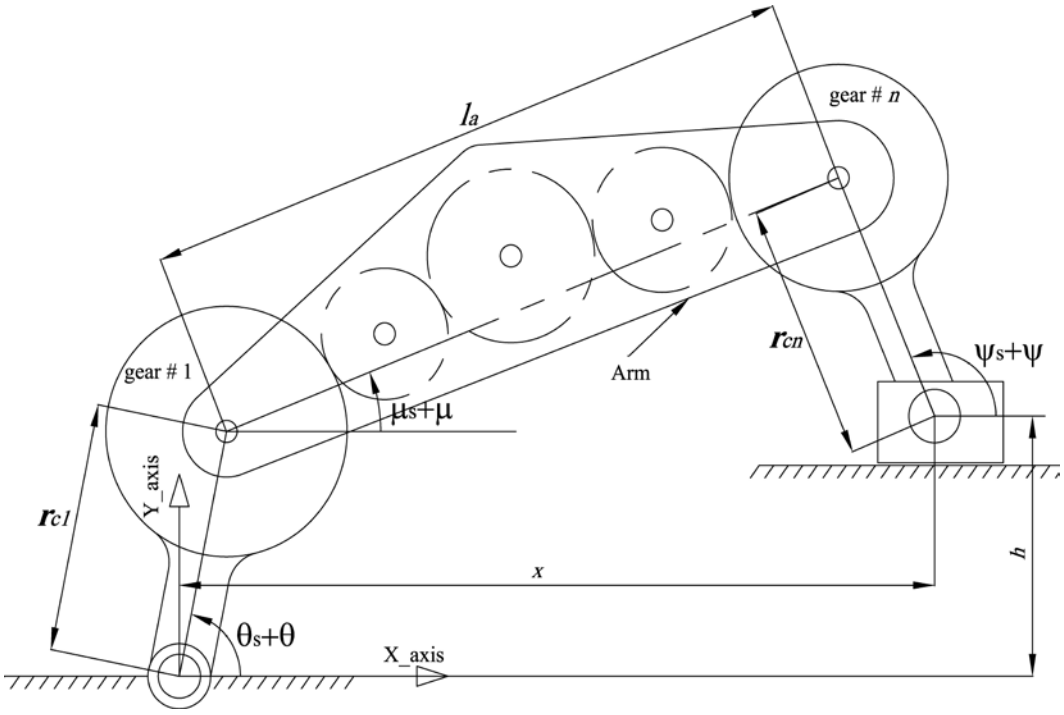

Figure 2.2 Geared five-bar slider-crank mechanism

As shown in Figure 2.2, the geared five-bar slider-crank mechanism consists of an epicyclic gear train on a triangular floating arm. The first gear 1 is pivoted to the origin of a Cartesian frame and the last gear n is connected to a sliding member through a rotary joint. Arm length is l_a and the distance from the centre to the pivot on first and last gears are r_{c1} and r_{cn} respectively. The overall gear ratio β may be expressed as:

$$\beta = (-1)^{n-1}\left(\frac{D_1}{D_n}\right) \qquad 2.9$$

where D_n is the pitch circle diameter of the last gear.

Equation 2.8 may be related as:

$$\frac{d\varphi}{dt} = (1-\beta)\frac{d\mu}{dt} + \beta\frac{d\theta}{dt} \qquad 2.10$$

where θ, μ and φ are angular displacements of the crank, the first gear, the arm and the last gear respectively. $\frac{d}{dt}$ in equation 2.10 represents differentiation with respect to time. Rearranging equation 2.10 to omit time:

$$\frac{d\varphi}{d\theta} = (1-\beta)\frac{d\mu}{d\theta} + \beta \qquad 2.11$$

Since at the assembly position, the three angular displacements θ, μ and φ are all set equal to 0, equation 2.11 may be integrated as:

$$\varphi = (1-\beta)\mu + \beta\theta \qquad 2.12$$

To this end, the geared five-bar slider-crank embodiments can be classified into Type-1 and Type-2 mechanisms. Type-1 design is dimensioned in such a manner that the arm can only rock through an angular span and the last gear can perform complete rotations. The Type-2 mechanism, on the other hand, is designed so that the arm can perform full rotations and the last gear can only perform rocking strokes. During the synthesis process as will be detailed in the next chapter, a design constraint will be employed to relate the three lengths, l_a, r_{c1} and r_{cn} in order for the optimization procedure to achieve either a Type-1 or a Type-2 design as desired.

In a Type-1 mechanism, the displacement μ is equal to 0 at both the start and the end of each cycle. In this case, φ is equal to 0 at the start of the work cycle, but at the end of the cycle φ is calculated from equation 2.12 as equal to $2\pi\beta\delta$. Since the

last gear will have to return to its original position at the end of the cycle, the product $\beta\delta$ is an integer. In fact, δ, which signifies the number of rotations performed by the first gear during one work cycle, is the smallest integer which makes the product of $\beta\delta$, also an integer. In order to calculate δ, the gear ratio β has to be expressed in a simplified fractional form rather than in a decimal from.

In Type-2 mechanisms, the displacement φ is equal to 0 at both the start and end of each cycle. The arm displacement, μ is equal to 0 at the start of the work cycle, but at the end of the cycle it is calculated from equation 2.12 as equal to $\frac{2\pi\beta\delta}{(\beta-1)}$, where $\beta \neq 1$. The arm has to return to its original position suggests that the product of $\frac{\beta\delta}{(\beta-1)}$ is also an integer. Designs in which β is set equal to 1 produce Type-1 mechanism since equation 2.12 will be reduced to $\varphi = \theta$ all through the cycle. However, such a mathematical simplicity is likely to reduce the ability of the mechanism to conform to some special stroke requirements if stipulated by design.

From Figure 2, the instantaneous x-coordinate of the slider pivot, x, and its constant y-coordinate, h, may be expressed as:

$$x = r_{c1}Cos(\theta_s + \theta) + l_a Cos(\mu_s + \mu) - r_{cn}Cos(\varphi_s + \varphi) \qquad 2.13$$

and

$$h = r_{c1}Sin(\theta_s + \theta) + l_a Sin(\mu_s + \mu) - r_{cn}Sin(\varphi_s + \varphi) \qquad 2.14$$

The values of the link angles, θ_s, μ_s and φ_s are defined by the synthesis procedure and are used to position the various links during assembly.

2.4 NUMERICAL KINEMATIC SOLUTION

The solution presented here is a differential-model-based numerical procedure carried out to calculate the positions of various links against infinitesimal progression of an input displacement. The differential model for geared five-bar mechanism may be obtained by differentiating equations 2.13 and 2.14 with respect to θ:

$$\frac{dx}{d\theta} = -r_{c1}Sin(\theta_s + \theta) - l_a Sin(\mu_s + \mu)\frac{d\mu}{d\theta} - r_{cn}Sin(\varphi_s + \varphi)\frac{d\varphi}{d\theta} \qquad 2.15$$

and

$$0 = r_{c1}Cos(\theta_s + \theta) + l_a Cos(\mu_s + \mu)\frac{d\mu}{d\theta} - r_{cn}Cos(\varphi_s + \varphi)\frac{d\varphi}{d\theta} \qquad 2.16$$

The set of ordinary differential equations 2.11, 2.15 and 2.16 can be solved numerically using Euler's forward method. For this procedure, the cyclical motion of the input link is divided in L infinitesimal jumps; where L is selected large enough to ensure a desired level of accuracy. At step number i, the displacement, δx_i, $\delta\mu_i$ and $\delta\varphi_i$ corresponding to a given value of infinitesimal displacement, $\delta\theta$ (where $\delta\theta = \frac{2\pi\delta}{L}$) may be obtained as:

$$J_{\theta i}\begin{bmatrix}\delta x_i \\ \delta\mu_i \\ \delta\varphi_i\end{bmatrix} = \begin{bmatrix} r_{c1}Sin(\theta_s + \theta_i) \\ -r_{c1}Cos(\theta_s + \theta_i) \\ -\beta \end{bmatrix}\delta\theta \qquad 2.17$$

where θ_i is the value of the crank displacement, θ, at step number i and the kinematic Jacobian, $J_{\theta i}$, is expressed as:

$$J_{\theta i}=\begin{bmatrix} -1 & -l_a Sin(\mu_s+\mu_i) & r_{cn}Sin(\varphi_s+\varphi_i) \\ 0 & l_a Cos(\mu_s+\mu_i) & -r_{cn}Cos(\varphi_s+\varphi_i) \\ 0 & 1-\beta & -1 \end{bmatrix} \qquad 2.18$$

where μ_i and φ_i are the values of μ and φ respectively at step number i_i. Condition of the mechanism when it does not run singularity is seizure or bifurcation as:

$$\left|J_{\theta i}\right| = l_a Cos(\mu_s+\mu_i) - r_{cn}(1-\beta)Cos(\varphi_s+\varphi_i) \neq 0 \qquad 2.19$$

If β was set equal to 1, the condition for non-singularity is $\frac{\pi}{2} \geq \mu_s + \mu \geq -\frac{\pi}{2}$ meaning that Type-1 mechanism has been concluded earlier. The updated value of the total displacement of the link at the start of step number $i+1$ may be calculated as:

$$\left.\begin{aligned} \theta_{i+1} &= \theta_i + \delta\theta_i \\ x_{i+1} &= x_i + \delta x_i \\ \mu_{i+1} &= \mu_i + \delta\mu_i \\ \varphi_{i+1} &= \varphi_i + \delta\varphi_i \end{aligned}\right\} \qquad 2.20$$

In order to find a mathematical condition to determine as to whether the slider is at one of its stationary positions, it would be possible to set equation 2.15 equal to 0. However, the resulting expression would feature differential quantities which substituted by functional forms, will incur divisions by the determinant of matrix $J_{\theta i}$. To avoid numerical complications, it is possible to rearrange equation 2.17 in the following form:

$$J_{\theta i}\begin{bmatrix} \delta\theta_i \\ \delta\mu_i \\ \delta\varphi_i \end{bmatrix} = \begin{bmatrix} \delta x_i \\ 0 \\ 0 \end{bmatrix} \qquad 2.21$$

where the matrix J_{xi} is another kinematic Jacobian for the mechanism, and it may be expressed as:

$$J_{xi} = \begin{bmatrix} -r_{c1}Sin(\theta_s + \theta_i) & -l_a Sin(\mu_s + \mu_i) & r_{cn}Sin(\varphi_s + \varphi_i) \\ r_{c1}Cos(\theta_s + \theta_i) & l_a Cos(\mu_s + \mu_i) & -r_{cn}Cos(\varphi_s + \varphi_i) \\ \beta & 1-\beta & -1 \end{bmatrix} \qquad 2.22$$

For the slider to be stationary, the determinant of the matrix J_{xi} has to vanish. At step number i, this determinant can be simplified as:

$$\begin{aligned} \left|J_{xi}\right| = \; & l_a r_{cn}\beta Sin(\mu_s + \mu_i - \varphi_s - \varphi_i) \\ & - l_a r_{c1} Sin(\mu_s + \mu_i - \theta_s - \theta_i) \\ & + r_{cn} r_{c1}(1-\beta) Sin(\varphi_s + \varphi_i - \theta_s - \theta_i) \end{aligned} \qquad 2.23$$

Instantaneous velocities:

$$\left.\begin{aligned} \overset{\circ}{x}_i &= \delta x_i / \delta t \\ \overset{\circ}{\mu}_i &= \delta \mu_i / \delta t \\ \overset{\circ}{\phi}_i &= \delta \phi_i / \delta t \end{aligned}\right\} \qquad 2.24$$

where $\overset{\circ}{x}_i$, $\overset{\circ}{\mu}_i$ and $\overset{\circ}{\phi}_i$ are the velocities of the slider, arm and last gear respectively. In equation 2.24, δt (where $\delta t = \frac{\delta\theta}{\omega_1}$) is the infinitesimal time period over which $\delta\theta$ occurs.

Also the instantaneous accelerations $\overset{\circ\circ}{x}_i$, $\overset{\circ\circ}{\mu}_i$ and $\overset{\circ\circ}{\phi}_i$ of the slider, arm and last gear respectively are as given below:

$$\left.\begin{aligned} \overset{\circ\circ}{x}_i &= \left(\delta x_{i+1} - \delta x_i\right) \Big/ \delta t^2 \\ \overset{\circ\circ}{\mu}_i &= \left(\delta \mu_{i+1} - \delta \mu_i\right) \Big/ \delta t^2 \\ \overset{\circ\circ}{\phi}_i &= \left(\delta \phi_{i+1} - \delta \phi_i\right) \Big/ \delta t^2 \end{aligned}\right\} \qquad 2.25$$

If acceleration analysis is required, an extra step has to be added to the computational kinematics to obtain position data at step number L.

Chapter 3

Kinematic Synthesis of the Geared Five-Bar Slider Crank Mechanism for Positive Displacement Machinery

3.1 INTRODUCTION

The design process of mechanical linkages conventionally features two main activities. First, a 'type synthesis' is undertaken to select the type and number of joints and links used for the mechanism. Then 'dimensional synthesis' is carried out to calculate the lengths of various links used which ensure that a point on the output link will pass via a set of 'precision' points during the periodic motion of the mechanism. For a small number of precision points, closed form mathematical analysis can be conducted to find the main dimensions of the mechanism. Examples of this synthesis can be found in the work of Haung and Roth (1993) that combines the geometric constraints with static force equations for the analysis. However, the availability of the computing resources and optimization techniques has encouraged the effort to design linkages capable of following curves and functions, thus transforming the synthesis task to different domain. An excellent account of how optimization techniques have been introduced into the field of mechanism synthesis is given by Gabrielle (1993). Zhang et al (2000) present an interesting paper which

features direct application of the optimization theory in the field of mechanism synthesis.

Although optimization has introduced novel numerical tools into the field of mechanism design, yet it has also some mathematical difficulties inherent to this specific field. For example, the geometric constraints of a given mechanism have to adversely reflect on its ability to perfectly follow a specific curve. Also non-assembly solutions, obtained during an iterative procedure, often result in singularities and numerical inabilities as pointed out by Cossalter et al (1992). Non-assembly has been given a special focus by Minaar et al (2001) who used multi-body formulation and gradient-based optimization technique for mechanism synthesis. Their approach has been echoed by Jensen and Hansen (2006). However, Hansen (2002) inserts fictitious joints and links on the mechanism structure to increase the mobility during the optimization procedure. This is likely to reduce numerical inabilities which result from non-assembly. Deb and Tiwari (2005) and Cabera et al (2002) proposed Genetic Algorithm (GA) used for the synthesis problems. Tabu search is a simulation-based search technique which has successfully been used by Smaili et al (2005) for mechanism design. The work by Dooner (2001) features the combination of the two four-bar chains in a fashion that will produce a degree of mobility suitable for the path following the application.

A geared five-bar mechanism has been synthesized by Nokleby and Podhorodeski (2001) who employed Grashoff's condition, an elegant technique to transform the constraint optimization problem into a non-constraint one. The papers of Suchora and Savage (1974a and 1974b) represent the earliest in depth effort in the area of

five-bar geared mechanism. The focus of the work by Suchora and Savage was the embodiment in which the first gear is stationary. In this thesis the focus is on the version in which the last gear is attached to a sliding element. A version of this embodiment was patented by Bresland (2001) as a drive mechanism for internal combustion engines. The slider can be employed as a piston in a reciprocating positive displacement machine to utilize the ability of five-bar geared mechanism to offer such aspects as multiple stroke lengths and dwells. In a positive displacement machine, these aspects can be used to increase efficiencies (volumetric and thermal) and reduce flywheel size and associated dynamical effects. Multi-section synthetic curves will be used, in this work, to guide the motion of the piston but point-to-point matching is not required except at stroke ends and dwells, which are regarded as precision points. At these points, both the position and velocity values obtainable by the designed mechanism are expected to match the corresponding values given by the synthetic curve as will be shown in the examples given at the end of the chapter. The next section presents the kinematic aspects of the geared five-bar slider-crank mechanism.

3.2 MECHANISM SYNTHESIS

The particulars of the desired piston trajectory may have to be decided by the designer before employing synthesis procedure, in order to design a geared five-bar slider-crank mechanism. These particulars are mainly the lengths of various strokes, the crank angle which corresponds to each stroke and the number of crank rotations which correspond to one cycle of the machine operation. Based on these particulars, a numerical procedure is adopted to calculate a design vector $[\theta_s \;\; \mu_s \;\; \varphi_s \;\; r_{c1} \;\; r_{cn} \;\; l_a]^T$, that will, as much as possible, realize the desired trajectory particulars. It should be

noted that ‘ h ’ has not been included in the design vector since it can be calculated by re-writing equation 2.14 at the assembly position as follows:

$$h = r_{c1}Sin(\theta_s) + l_a Sin(\mu_s) - r_{cn}Sin(\varphi_s) \qquad 3.1$$

The approach used in this thesis features the construction of a multi-section guiding curve which combines the characteristics of each stroke. Examples of the construct which may be used to synthesize this curve are given in the cosine functions, cycloidal functions and cubic splines. Mathematical representation of these constructs are given in Appendix A.

On the guiding curve, the ‘M’ timing points, at which the slope vanishes, correspond to the end of piston strokes. These timing terminals are chosen as precision points at which high weighting values will be given to both the distance-based objective functions and velocity constraints. The other points of the curve are used only to ‘guide’ the direction on which the piston should move.

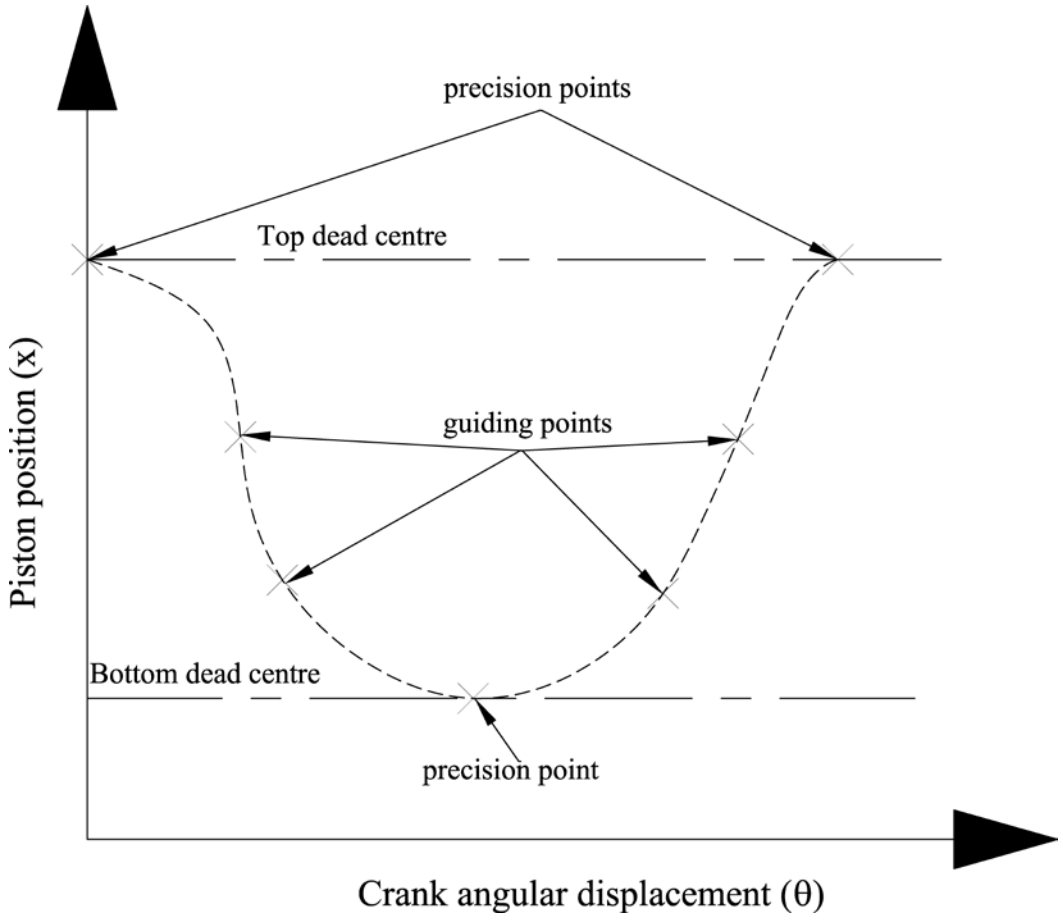

Figure 3.1 The concept of the Guiding Curve

In the procedure presented in this thesis, the total number of points on the curve is 'N'; and the points for every stroke can be spaced out either equally or by using Chebyshev series. Figure 3.1 depicts a possible such curve as employed for the synthesis procedure.

The zero-valued distance-based objective function, f_{xq}, which should be minimized is expressed in reference to equation 2.13 as follows:

$$f_{xq} = r_{c1}Cos(\theta_s + \theta_q) + l_a Cos(\mu_s + \mu_q) - r_{cn}Cos(\varphi_s + \varphi_q) - x_{gq} \qquad 3.2$$

where $q = 0 \ldots N–1$ and x_{gq} is the x-coordinate of point number q on the guiding curve.

The minimization process is subject to the equality constraints, g_{vj} (where $j = 0 \ldots M–1$), which are introduced to ensure compliance with stroke timing requirements as:

$$\begin{aligned} g_{vj} = & -l_a r_{c1} Sin(\mu_s + \mu_j - \theta_s - \theta_j) \\ & + l_a r_{cn} \beta Sin(\mu_s + \mu_j - \varphi_s - \varphi_j) \\ & + r_{c1} r_{cn} (1-\beta) Sin(\varphi_s + \varphi_j - \theta_s - \theta_j) \end{aligned} \qquad 3.3$$

The optimized solution is also subject to the following mobility constraint:

$$\prod_{q=o}^{N-1} \left[l_a Cos(\mu_s + \mu_q) - r_{cn}(1-\beta) Cos(\varphi_s + \varphi_q) \right] \geq 0 \qquad 3.4$$

where $N-1$ is assumed to be an odd number. However, $N-1$ is usually calculated by dividing the cyclical angular displacement of the crank by a desired angular interval. Thus, if $N-1$ has been found to be an even number at the start of numerical procedure, the consecutive multiplications in the equation 3.4 may be taken up to $N-2$ terms in order to ensure a positive product.

The following three constraints have been introduced to impose minimum or maximum limits on dimensions;

$$\left(r_{c1} Sin(\theta_s) + l_a Sin(\mu_s) - r_{cn} Sin(\varphi_s) \right)^2 - h_{\max}^2 \leq 0 \qquad 3.5$$

$$r_{c1} - r_{c1\min} \geq 0 \qquad 3.6$$

$$r_{cn} - r_{cn\min} \geq 0 \qquad 3.7$$

where $h_{\max}$, $r_{c1\min}$ and $r_{cn\min}$ are numbers employed to signify the limits imposed on their respective dimensions.

Inequality 3.7 is used for only Type-1 mechanism, for a Type-2 mechanism this inequality is replaced by $l_a - l_{a\min} \geq 0$, where $l_{a\min}$ is the minimum allowable arm length. Moreover, the following constraint has been employed to make sure that the arm length is large enough to ensure limited angular stroke for the arm in Type-1 mechanism;

$$l_a - \sqrt{{r_{c1}}^2 - {r_{cn}}^2} \geq 0 \qquad 3.8$$

where for a Type-2 mechanism, this inequality is replaced by

$$r_{cn} - \sqrt{{r_{c1}}^2 - {l_a}^2} \geq 0$$

Antoniou and Lu (2007) suggest that inequality constraint can be transformed into equality constraint function g_m, g_h, g_{c1}, g_{cn} and g_l, by introducing a set of 'slack variables' as:

$$\left.\begin{aligned} g_m &= \prod_{q=o}^{N-1}\left[l_a Cos(\mu_s+\mu_q) - r_{cn}(1-\beta)Cos(\varphi_s+\varphi_q)\right] - a_m^2 = 0 \\ g_h &= \left(r_{c1}Sin(\theta_s) + l_a Sin(\mu_s) - r_{cn}Sin(\theta_s)\right)^2 - h_{\max}^2 - a_h^2 = 0 \\ g_{c1} &= r_{c1} - r_{c1\min} - a_{c1}^2 = 0 \\ g_{cn} &= r_{cn} - r_{cn\min} - a_{cn}^2 = 0 \\ g_l &= l_a - \sqrt{r_{c1}^2 - r_{cn}^2} - a_l^2 = 0 \end{aligned}\right\} \qquad 3.9$$

The slack variables, a_m, a_h, a_{rc1}, a_{rcn} and a_l featured in 3.9 will result in an augmented design vector:

$$\mathbf{V} = \left[\theta_s \;\; \mu_s \;\; \phi_s \;\; r_{c1} \;\; r_{cn} \;\; l_a \;\; a_m \;\; a_h \;\; a_{rc1} \;\; a_{rcn} \;\; a_l\right]^T$$

It is worthy of noting here that the set of equation 3.9 is written for Type-1 mechanism. For Type-2 mechanism, the bottom two equations in the set are replaced by the following:

$$\left.\begin{aligned} g_{cn} &= r_{cn} - \sqrt{r_{c1}{}^2 - l_a{}^2} - a_{cn}^2 = 0 \\ g_l &= l_a - l_{a\,\min} - a_l^2 = 0 \end{aligned}\right\} \qquad 3.10$$

The next section presents the details of the mathematical implementation of the mechanism synthesis model.

3.3 COMPUTATIONAL PROCEDURE

The gradient-based technique employed in this chapter features a Marquadt-Levenberg formulation where the vector, **e** is given in relation to the expression detailed in 3.2, 3.3, 3.9 and 3.10 as:

$$\mathbf{e} = \left[\, f_{x0} \cdots f_{xN-1} \;\; g_{v0} \cdots g_{vM-1} \; g_m \;\; g_h \;\; g_{rc1} \;\; g_{rcn} \;\; g_l \right] \qquad 3.11$$

The Marquadt- Levenberg formula has been chosen for this analysis because it is robust and offers a damping factor which can be used to control the speed of convergence. In numerically unstable problems, such as mechanism synthesis, this aspect is very useful. During iterations, **e** is updated and employed to calculate the design vector correction, $\boldsymbol{\delta}\mathbf{V}$. This process involves the use of the system Jacobian, $\mathbf{J}$, whose entries are partial derivatives, of the functions which constitute the vector $\mathbf{e}$.

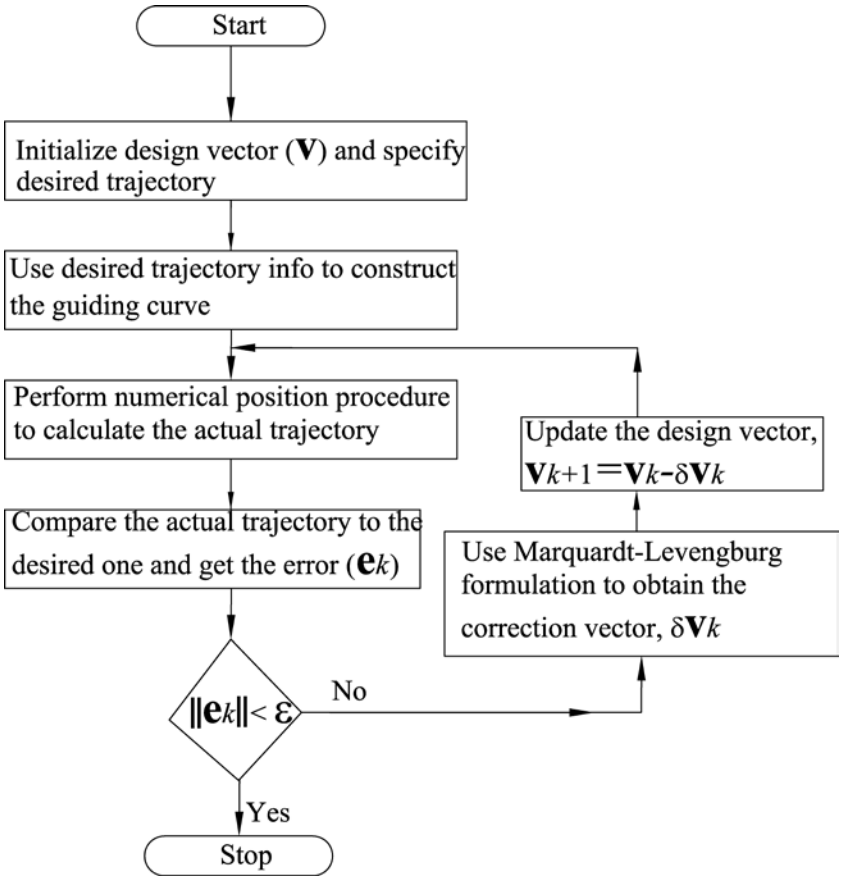

Figure 3.2 Flowchart for the mechanism synthesis procedure

As summarised by the flowchart given in Figure 3.2, convergence is assessed at iteration number k by the most updated error vector, $\mathbf{e}_k$ (i.e. $\|\mathbf{e}_k\| \le \varepsilon$, where $\|\bullet\|$ indicates the Euclidean norm and ε is a small positive number). If convergence has not been achieved, the iterative process continues using the following expression;

$$\boldsymbol{\delta}\mathbf{V}_k = (\mathbf{J}_k^T \mathbf{W} \mathbf{J}_k + \lambda \mathbf{I})^{-1} \mathbf{J}_k^T \mathbf{W} \mathbf{e}_k \qquad 3.12$$

where $\mathbf{J}_k$ and $\boldsymbol{\delta}\mathbf{V}_k$ are updated values of $\mathbf{J}$ and $\boldsymbol{\delta}\mathbf{V}$, respectively, at iteration number k. In equation 3.12, $\mathbf{W}$ is a diagonal matrix whose positive entries are chosen to reflect the weighting which every function should have on the resulting solution. This matrix has been used to distinguish the stationary points (i.e., the precision points) from the point which are only used to guide the direction of the piston motion. The identity matrix, $\mathbf{I}$, in equation 3.12 is of dimension 11x11 and λ

is a positive real number damping factor which is initially assigned a large value. This value is then progressively reduced during iterations to regain the favourable convergence aspects of the Newton iterative technique. The rate at which λ is reduced during the iteration has to be fairly slow in order for useful solution points to be captured by the procedure. This is needed to deal with the mathematical aspects of the mechanism synthesis problems, which often suffer from nonlinearly and non-assembly complications.

3.4 CASE STUDIES

Two case studies are presented in this chapter to prove the validity of the presented technique. For every case study Type-1 and Type-2 mechanisms will be synthesized in order to highlight the structural differences between the two types.

CASE STUDY-1

This case study has been inspired by Bresland (2001) who proposed utilizing the capabilities of the geared five-bar slider-crank mechanism for engine applications. For the case study an expanded stoke engine is being designed. The guiding curve has been synthesized using cosine functions to reflect the following particulars:

Crank revolutions per cycle (δ)	= 2
Crank angle assignment:	220° for the scavenging stroke
	140° for the induction stroke
	140° for the compression stroke

	220° for the expansion stroke
Short stroke length	= 20 mm (induction & compression)
Long stroke length	= 80 mm (expansion & scavenging)
x-coordinate at Top Dead Centre	= 100 mm
x-coordinate at Bottom Dead Centre	= 80 mm (for short stroke)
	20 mm (for long stroke)

TYPE-1 MECHANISM – CASE STUDY-1

The mechanism dimensions at the start of iterations are as follows:

$\theta_s = -90°$	$\varphi_s = 90°$	$\mu_s = 0°$
$r_{c1} = 20$ mm	$r_{cn} = 20$ mm	$l_a = 200$ mm

The gear ratio used for mechanism is ½ to ensure two revolutions per cycle, and a Chebyshev series was used to guide the piston motion.

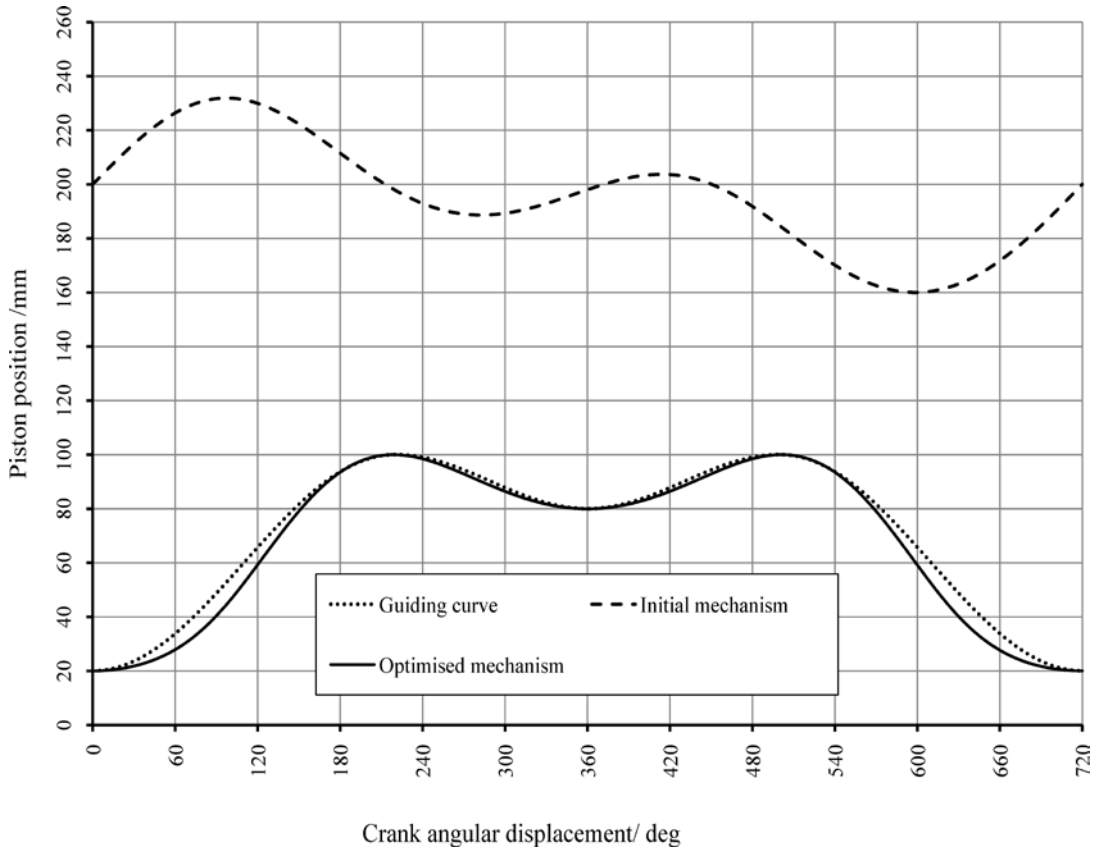

Figure 3.3 Piston trajectories for case study-1 (β = ½) Type-1 mechanism

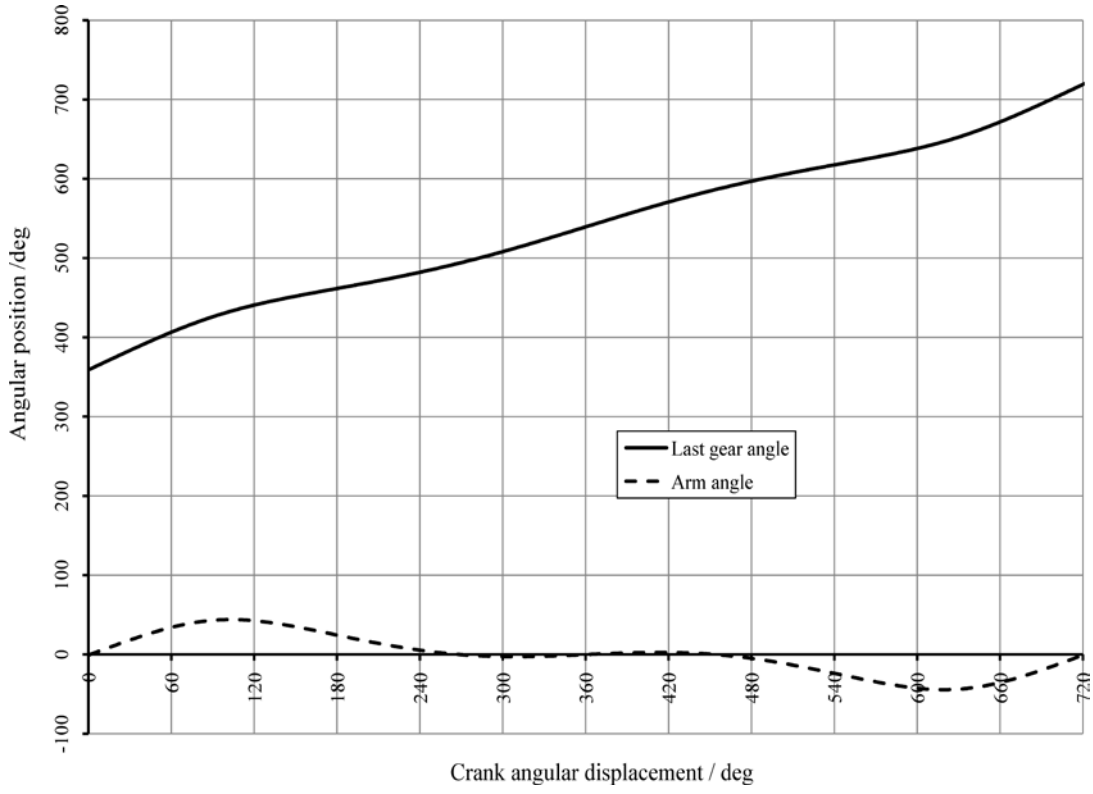

Figure 3.4 Arm and last gear position for case study-1 (β = ½) Type-1 mechanism

At the end of iterations, the produced piston trajectory as shown in Figure 3.3 along with guiding curve is used for analysis. The figure also shows the trajectory which corresponds to the initial values used for design parameter. Figure 3.4 is intended to show the angular stroke of the arm and continuous motion of the last gear. The resulting design parameters are given as follows:

$\theta_s = -179.5°$ $\varphi_s = 0.18°$

$h = -0.06$ mm $r_{c1} = 21.75$ mm $r_{cn} = 30$ mm $l_a = 71.72$ mm

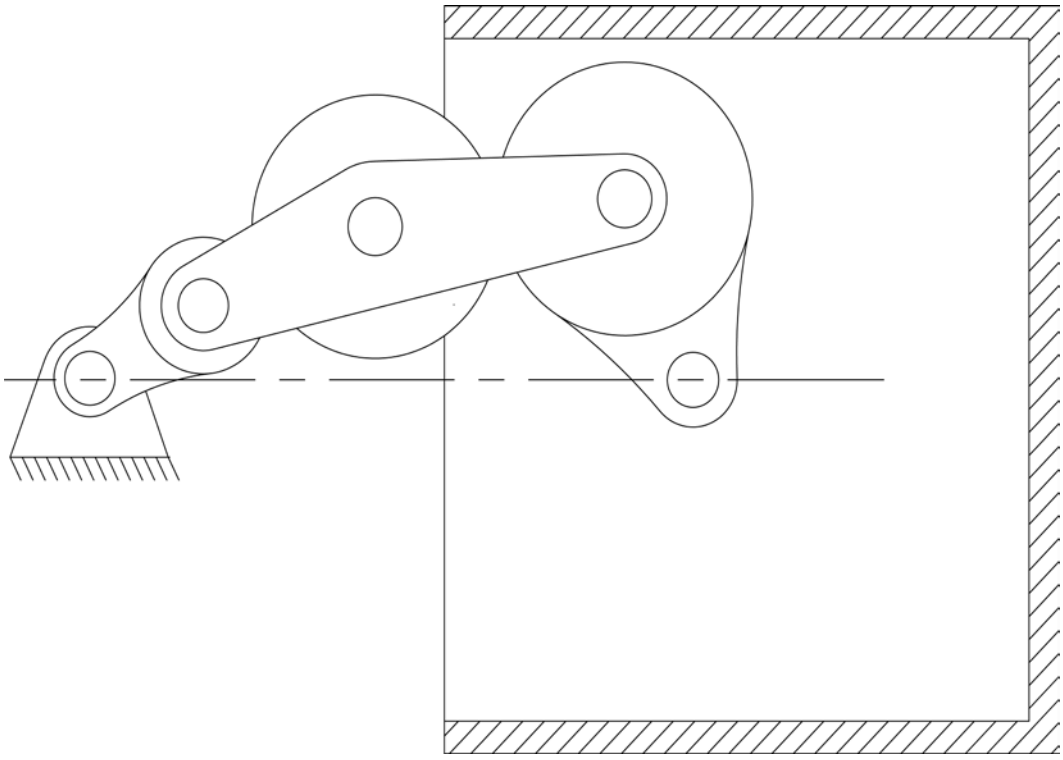

Figure 3.5 Rendering of the engine in case study-1 ($\beta = ½$) Type-1 mechanism

TYPE-2 MECHANISM – CASE STUDY-1

θ_s = 180° φ_s = 170° μ_s = 120°

r_{c1} = 20 mm r_{cn} = 80 mm l_a = 20 mm

The gear ratio for the mechanism is –1 to ensure two revolutions per cycle, and a Chebyshev series was used to guide the piston motion

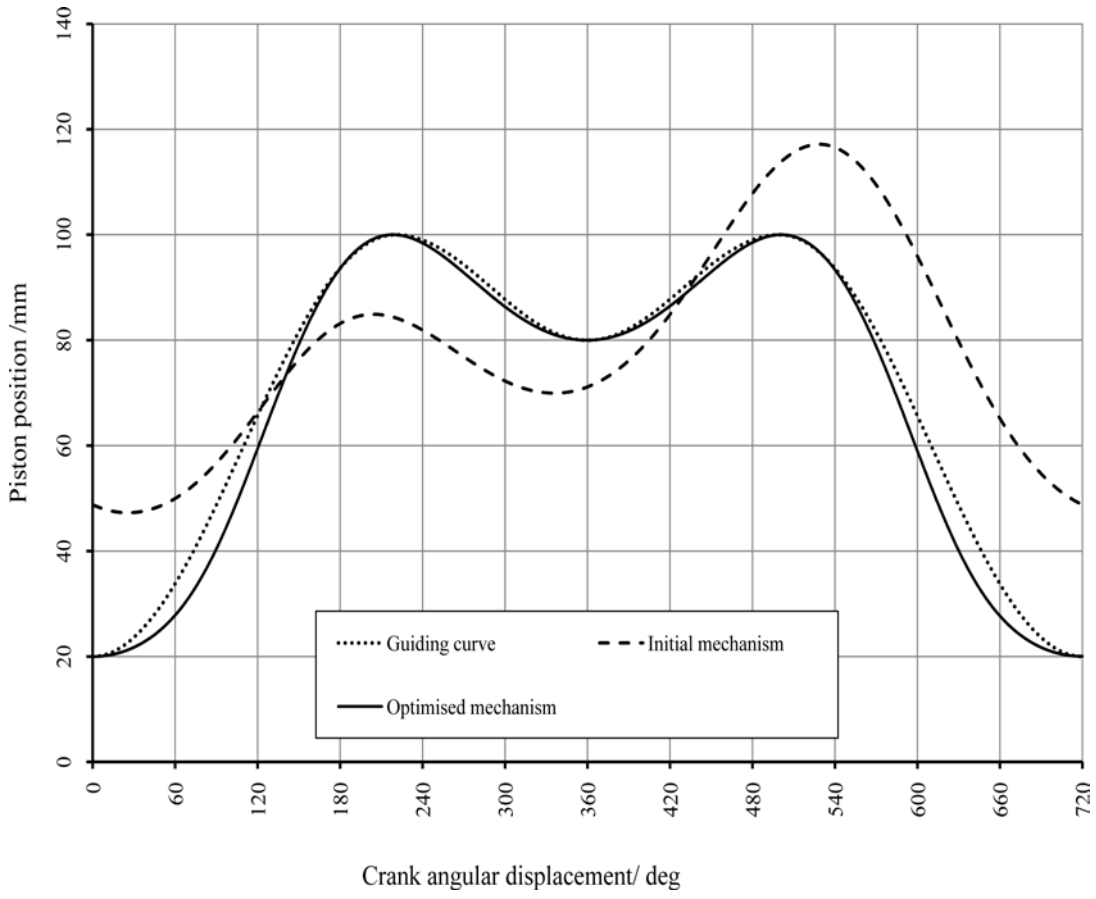

Figure 3.6 Piston trajectories for case study-1 (β = -1) Type-2 mechanism

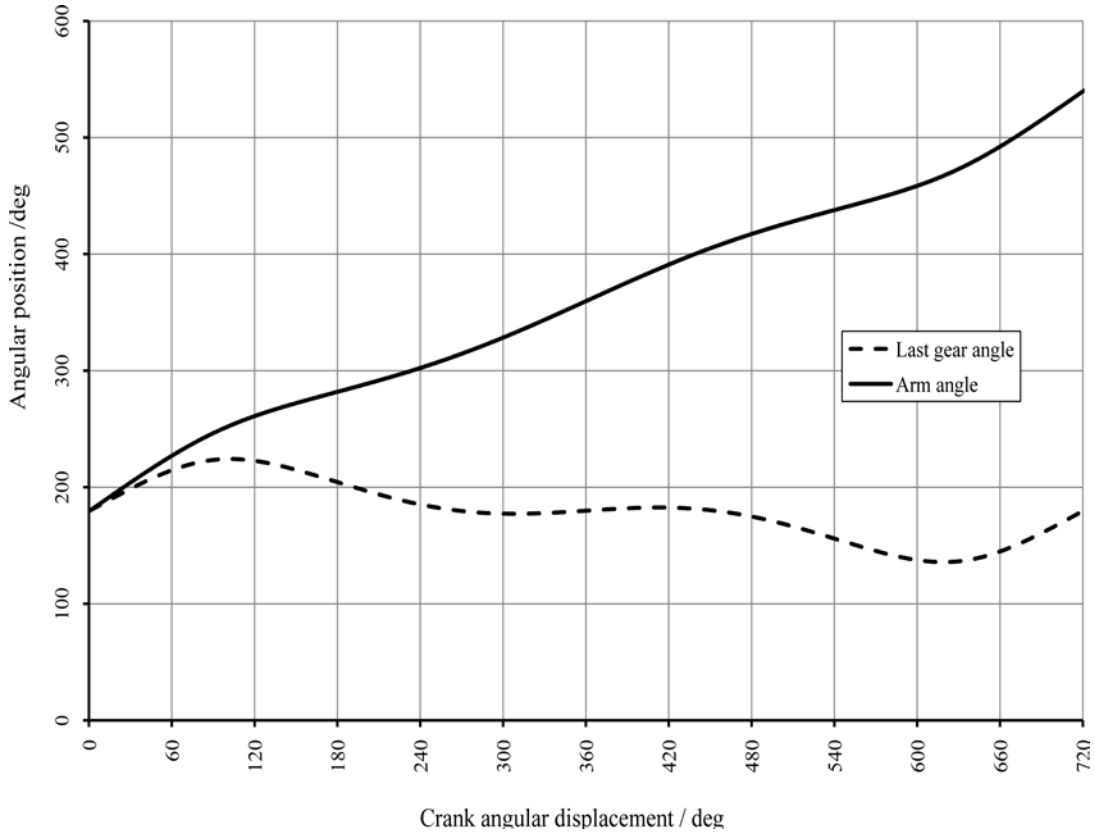

Figure 3.7 Arm and last gear positions for case study-1 (β = -1) Type-2 mechanism

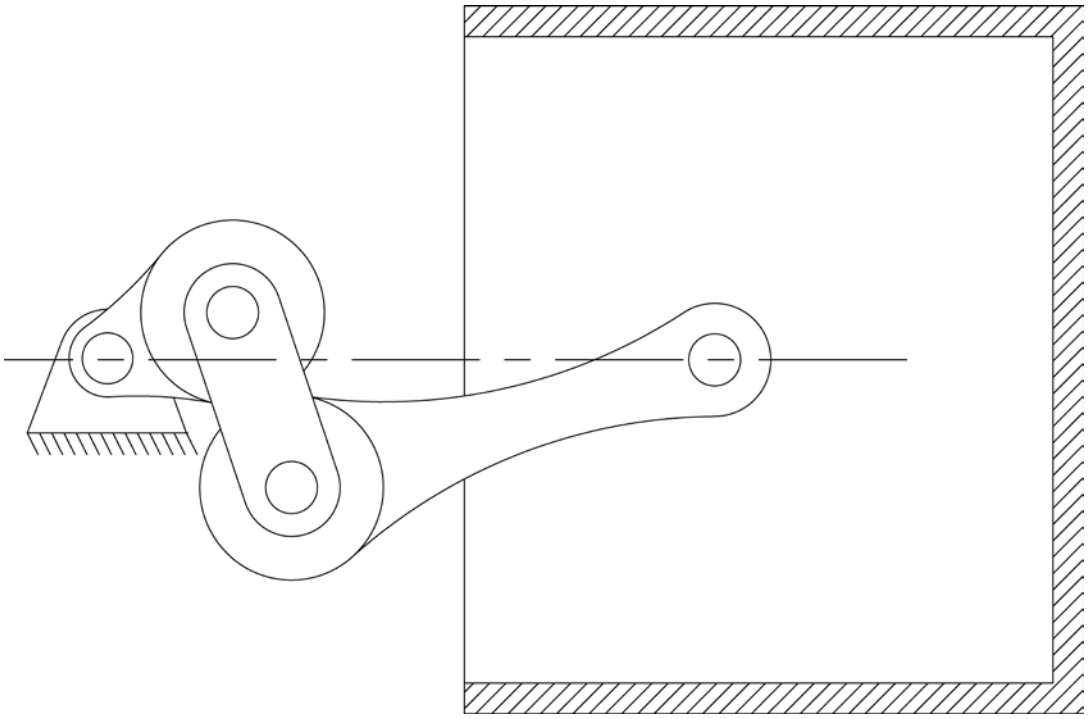

Figure 3.8 Rendering of the engine in case study-1 (β = -1) Type-2 mechanism

At the end of iterations, the produced piston trajectory is shown in Figure 3.6 along with the guiding curve used for analysis. The figure also shows the trajectory which corresponds to the initial value used for design parameters. Figure 3.7 shows the angular stroke of the last gear and the continuous motion of the arm. The resulting design parameters are given as:

θ_s = 180.4° φ_s = 180.31° μ_s = 180.37°

h = 0.04 mm r_{c1} = 21.75 mm r_{cn} = 71.72 mm

l_a = 30 mm

A scaled rendering of the optimized mechanism is shown in Figure 3.8.

Occasionally, it may not be possible to create a trajectory matching at the level shown by this case study. However, on these occasions, the optimization procedure will endeavour to produce the best possible matching mechanism as dictated by the constraints imposed by both the physical aspects of the linkage and design equations. For example, an attempt was made to re-design the Type-2 mechanism in case study 1 with the same motion particulars except the short stroke has been changed from 20 mm to 40 mm and gear ratio was set to 1/3 (which also produces two crank rotations per cycle). The result of the optimization is shown in Figure 3.9 which clearly indicated that the desired timing, on two occasions during the cycle, deviates considerably from the desired values. As such, another run was undertaken in which the weighting for the timing constraint was considerably increased. The outcome of this new run is shown in Figure 3.10 which suggests that an excellent timing match

was achieved but the stroke lengths have been compromised. In such a case the designer should endeavour to vary the weighting values given to various constraints in order for an acceptable result to be obtained. This acceptable solution would be a reasonable close alternative to what the designer had in mind at the start of the design process.

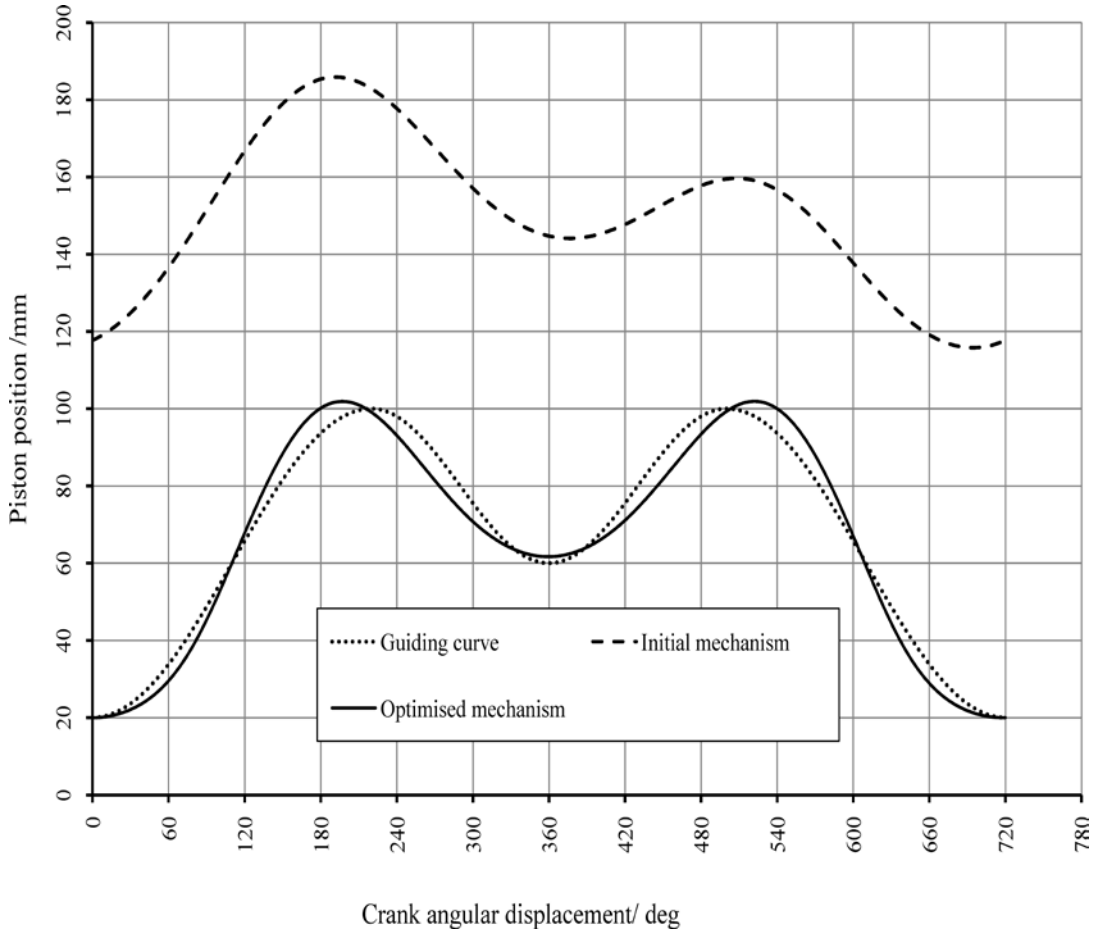

Figure 3.9 An optimized solution with timing deviation

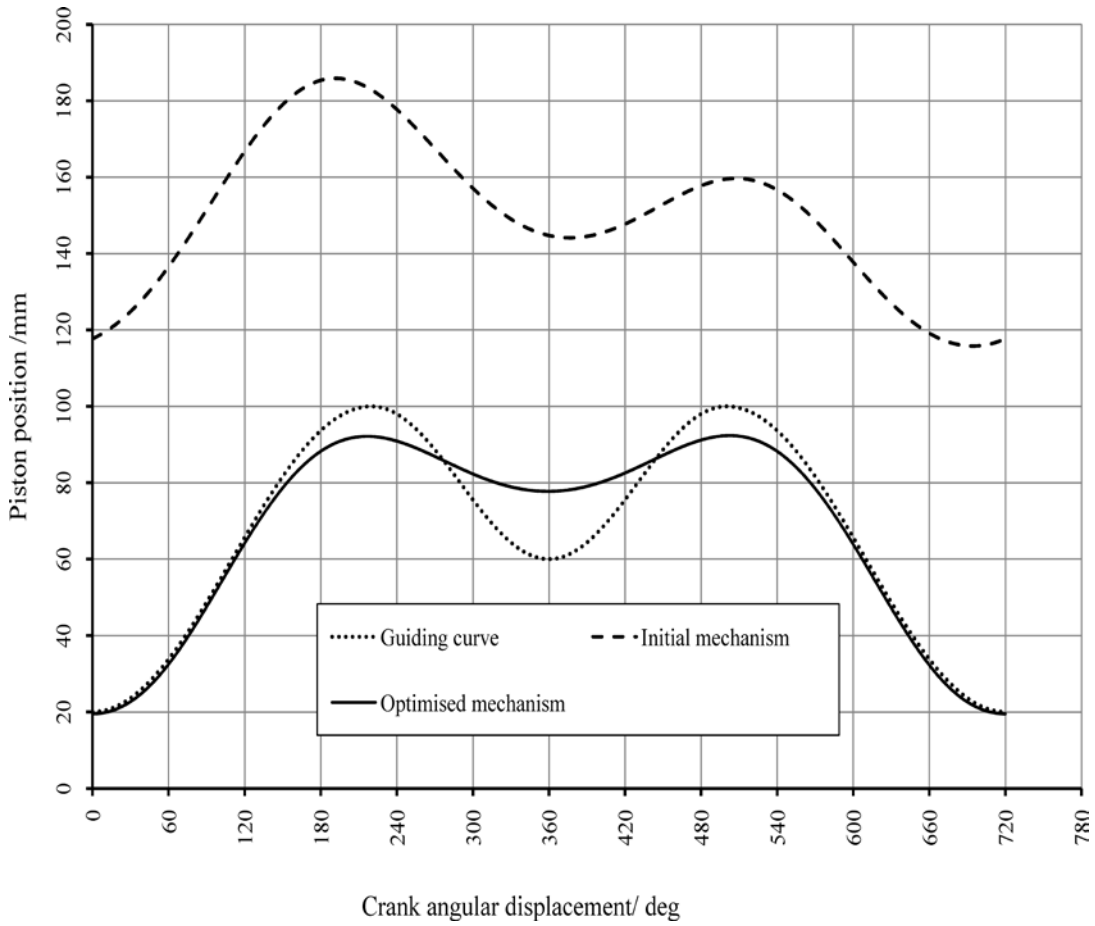

Figure 3.10 When high weighting is given to timing constraint g_{vj}.

CASE STUDY-2

This case study features the design of a reciprocating compressor. The guiding curve has been synthesized using cosine functions to reflect the following particulars:

Crank rotations per cycle (δ)	= 1
Crank angle assignment:	140° for the expansion stroke
	20° dwell
	220° for the compression stroke
Stroke length	= 100 mm

x-coordinate at Top Dead Centre = 200 mm

x-coordinate at Bottom Dead Centre = 100 mm

TYPE-1 MECHANISM – CASE STUDY-2

The mechanism dimensions at the start of iterations are as follows:

θ_s = 90° φ_s = 90° μ_s = 0°

r_{c1} = 20 mm r_{cn} = 20 mm l_a = 200 mm

The gear ratio, β, used for the mechanism is -1 to ensure one revolution per cycle.

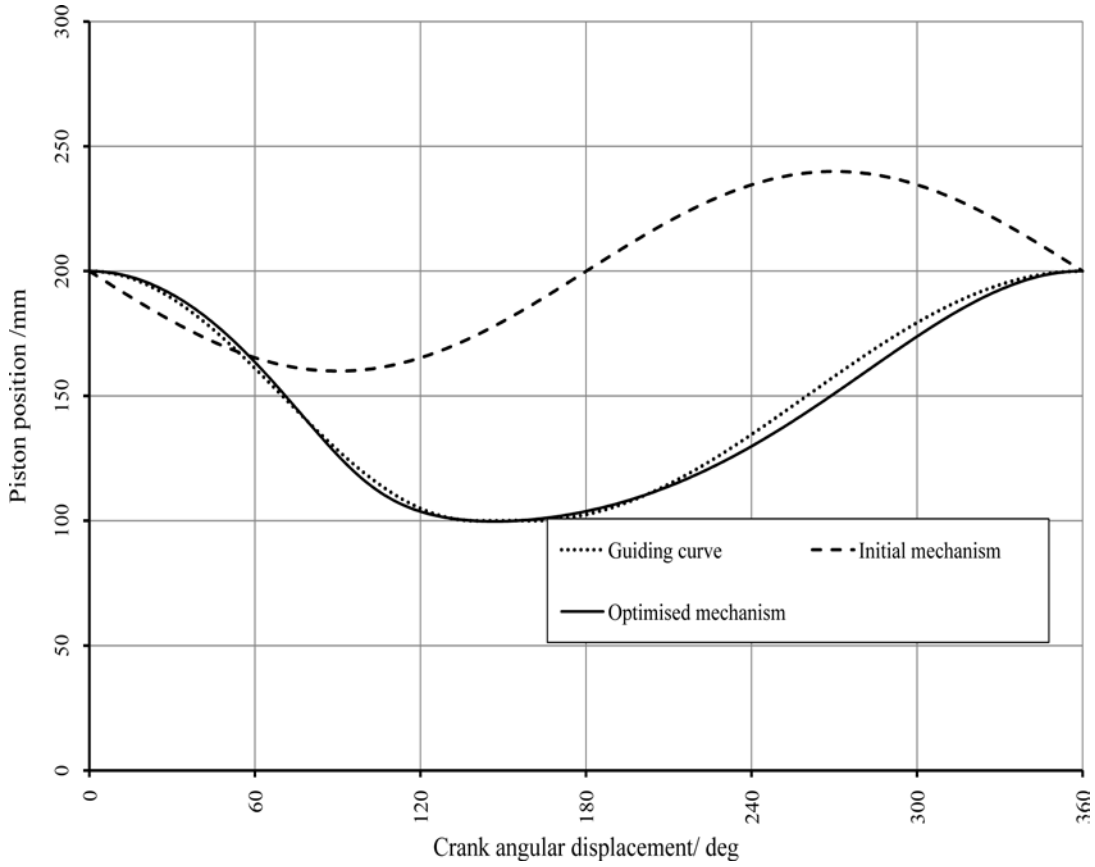

Figure 3.11 Piston trajectories for case study-2 (β = -1) Type-1 mechanism

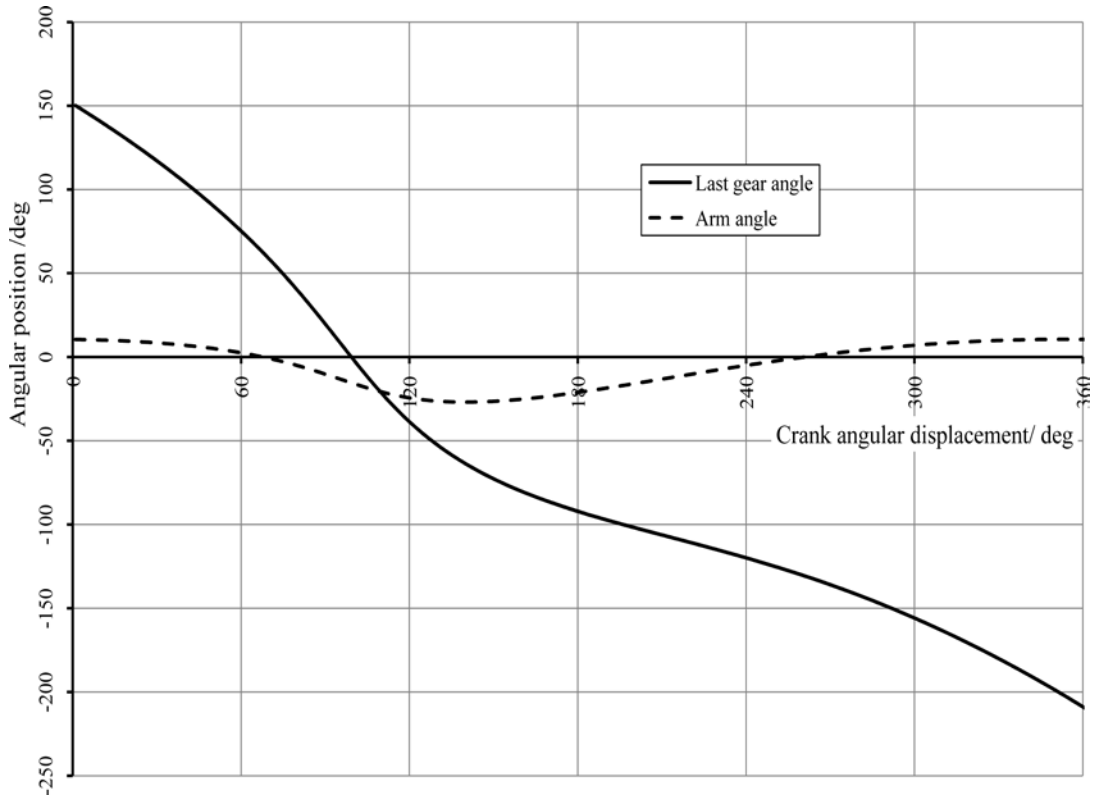

Figure 3.12 Arm and last gear positions for case study-2 (β = -1) Type-1 mechanism

At the end of iterations, the piston trajectory was produced as depicted in Figure 3.11 along with the guiding curve used for the analysis. The figure also shows the trajectory which corresponds to the initial values used for design parameters. Figure 3.12 is intended to show the angular stroke of the arm and the continuous motion of the last gear. During calculations a Chebyshev series was used to guide the piston motion. The resulting design parameters are as follows:

θ_s = –25.61° φ_s = 150.17° μ_s = 10.5°

h = –4.65 mm r_{c1} = 35.3 mm r_{cn} = 31.4 mm

l_a = 143.42 mm

A scaled rendering of the optimized mechanism is shown in Figure 3.13.

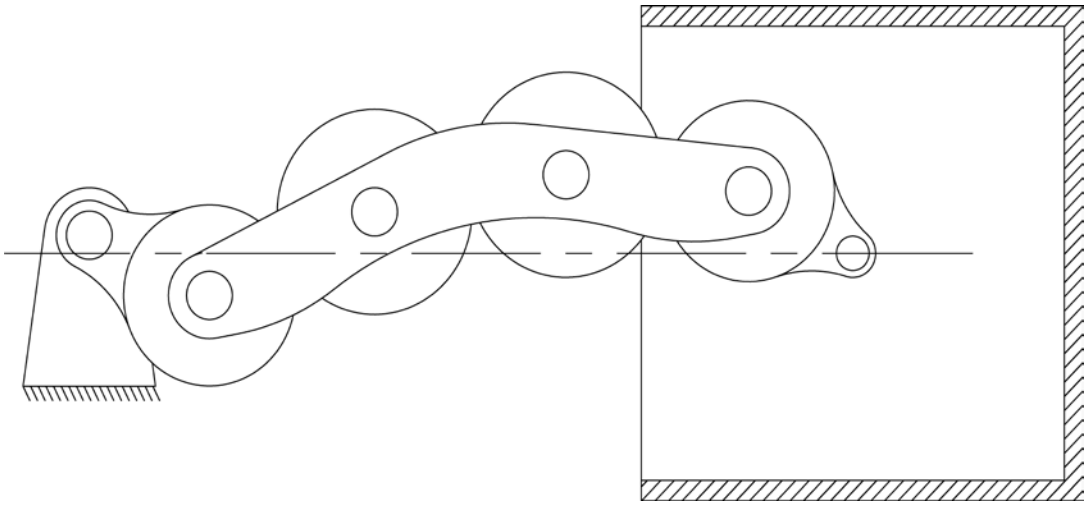

Figure 3.13 Rendering of the compressor in case study-2 (β = -1) Type-1 mechanism

TYPE-2 MECHANISM – CASE STUDY-2

θ_s = 120° φ_s = –90° μ_s = 0°

r_{c1} = 20 mm r_{cn} = 150 mm l_a = 20 mm

The gear ratio, β, used for the mechanism is ½ to ensure one revolution per cycle.

At the end of iterations, the piston trajectory was produced as depicted in Figure 3.14 along with the guiding curve used for the analysis. As shown in the figure, calculations started by an initial singular mechanism which still managed to converge to an acceptable solution.

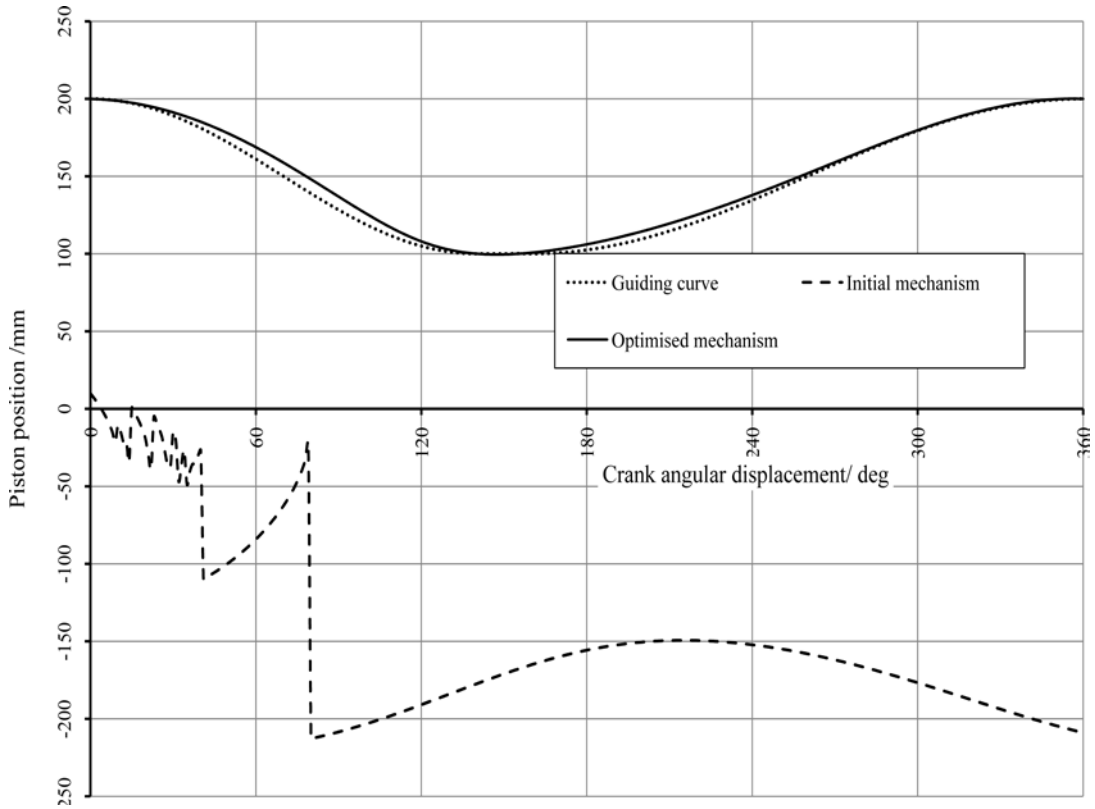

Figure 3.14 Piston trajectories for case study-2 (β = ½) Type-2 mechanism

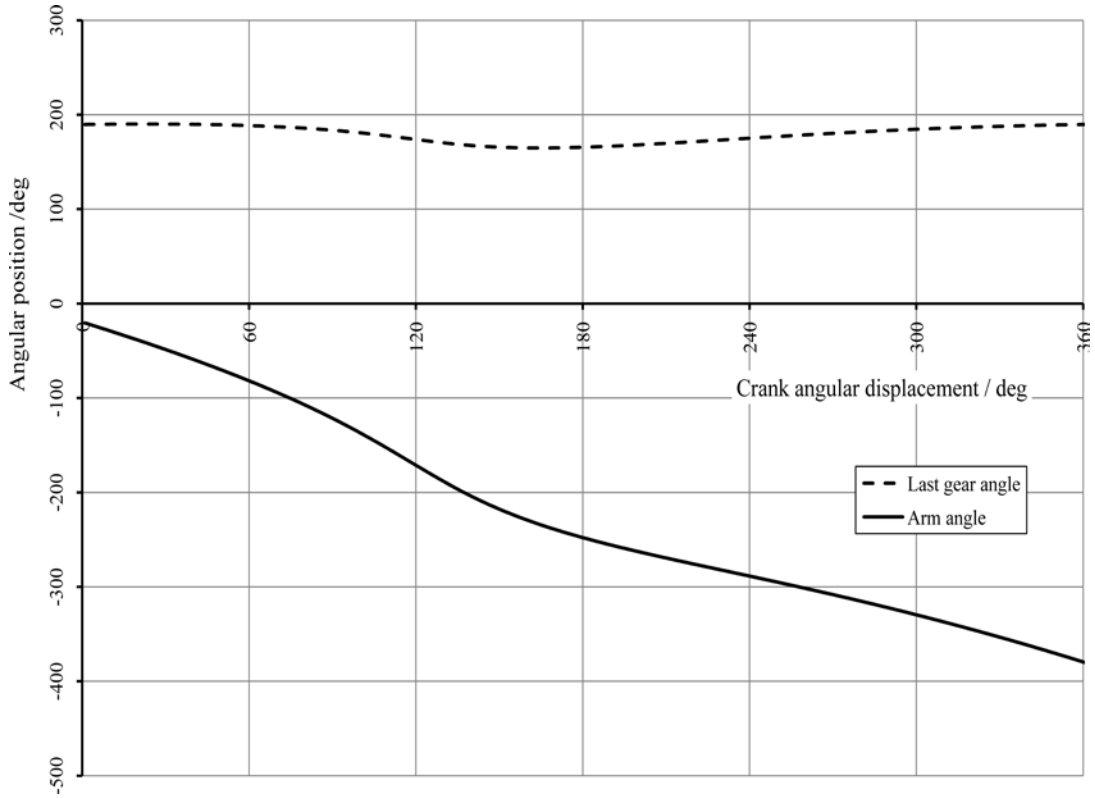

Figure 3.15 Arm and last gear positions for case study-2 (β = ½) Type-2 mechanism

Figure 3.15 shows the angular stroke of the last gear and the continuous motion of the arm. During calculations Chebyshev series was used to guide the piston motion. The resulting design parameters are as follows:

$\theta_s = -20.35°$ $\varphi_s = -189.67°$ $\mu_s = -20.48°$

$h = 3.94$ mm $r_{c1} = 23.25$ mm $r_{cn} = 146.69$ mm

$l_a = 33.87$ mm

A scaled rendering of the optimized mechanism is shown in Figure 3.1.

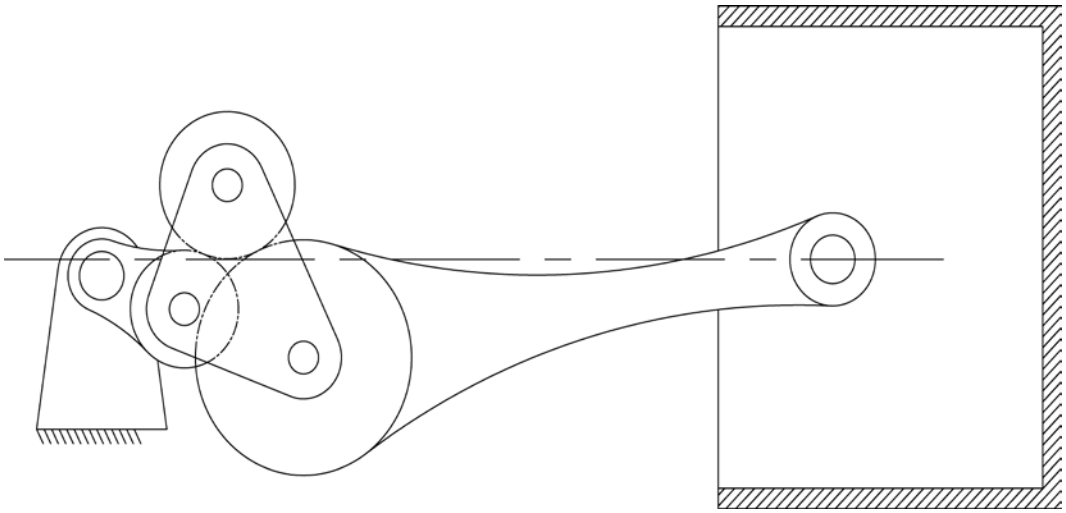

Figure 3.16 Rendering of the compressor in case study-2 ($\beta = ½$) Type-2 mechanism

Chapter 4

A Reciprocating Compressor based on the Geared Five-Bar Slider-Crank Mechanism

4.1 INTRODUCTION

In a reciprocating compressor, kinematic aspects such as dwell and stroke timing can be used to improve performance and reduce flywheel size and associated dynamical effects. The basic Premise in this chapter is that the geared five-bar slider-crank mechanism may be dimensioned in such a fashion that the kinematic particulars of the resulting stroke may result in optimised compressor performance. A vision that poses a two level-optimisation question: what are the optimum kinematic particulars and what are the dimensions which realize these particulars? In an attempt to answer these two questions the synthesis model, which has been presented in Chapter 3, will be coupled to differential thermodynamic model for the compressor embodiment.

In the work here, the stroke and the bore diameters will be kept constant during the optimisation procedure. So will the crank speed and the inlet and discharge pressures. As such, leakage will not be considered in the thermodynamic model employed for the analysis. This is unlike the approach adopted by Dagilis et al (2007) to optimise a conventional reciprocating design. In their approach, Dagilis et

al used the stroke-to-bore ratio as the design parameter to maximize a performance index defined as the ratio of the cooling capacity to the power consumption. In fact, the question of cooling and heat management does appear repeatedly in the published literature. Lekic and Kok (2008) highlight the importance of understanding the nature of the heat transfer process as they report the establishment of a highly advanced test rig, at the University of Twente, dedicated for that purpose. Their numerical results agree with those of Catto and Prata (2000) in the sense that both confirmed the notion that the temperature-time gradient of the compressed gas does affect the heat transfer process as does the temperature difference between the gas and cylinder wall. This is of particular importance to work proposed in this chapter because the temperature-time gradient is one aspect which the optimisation procedure presented will seek to reduce. This is likely to improve the ability of the cooling system to remove the heat generated during the compression stroke, which will result in reduced power consumption and more reliable operation.

The research of Stouffs et al (2001) features a creative effort to mathematically capture as much thermodynamic aspects as possible for reciprocating compressors. Their approach and mathematical models, which have been proven experimentally, will motivate future compressor studies. Rigola (2002) also presented a comprehensive in-depth study on the workings of compressors. More light was shed by Rigola et al (2004). A similar insightful effort into the workings of compressor values has been shown by Haping (2005). Understanding the dynamical and thermal aspects of these values is crucial for reliable performance.

A focus has been given to the mechanical aspects of reciprocating compressors by Estupinan and Santos (2007) who studied the dynamics of these fluid film lubrication in the crankshaft bearings. On the other hand Cho and Moon (2005) opted for investigating the effects of the oil film underlining the piston-cylinder interaction. Indeed the performance of these compressors is the result of intricate interactions of various mechanical and thermodynamic parameters as argued by Nietter and Singh (1984) who dedicated their paper to study the effects of the manifold acoustic aspects on the compressor efficiencies and pressure pulsations.

Published literature also does feature effort to investigate positive displacement compressor design other than the reciprocating ones. Peng et al (2002), for example, present a thermodynamic model for a novel rotary compressor design, and Sultan (2005 and 2006) proposes the use of the limacon machine for compression-expansion applications.

4.1 COMPRESSOR THERMODYNAMIC MODEL

For the thermodynamic model, a control volume is taken as the variable chamber volume entrapped by the piston cylinder arrangement. The confined volume of air, V_c, is calculated as follows:

$$V_c = V_{cl} + A_{cy}(x_{\max} - x) \qquad 4.1$$

where $x_{\max}$ denotes the piston x-coordinate as the Top Dead Centre (TDC), V_{cl} is the cylinder clearance volume and A_{cy} is the bore area. The rate, dm_c / dt, at which the

mass inside the control volume varies in relation to density and available space can be calculated from the following equation:

$$dm_c / dt = \omega\left[V_c\left(d\rho_c / d\theta\right) - A_{cy}\rho_c\left(dx / d\theta\right)\right] \qquad 4.2$$

where m_c and ρ_c are the mass and density of the fluid in the control volume respectively at any crank angle θ. In the model presented here $d\bullet/dt$ signifies derivative with respect to time and ω is a constant angular velocity given for the crank shaft rotations.

The continuity equation is expressed as follows:

$$dm_c / dt = Cd_i A_i \rho_c U_i - Cd_o A_o \rho_o U_o \qquad 4.3$$

where leakage is considered negligible and subscripts *i* and *o* refer to the inlet and outlet respectively. In the above equation, *Cd* denotes constant discharge coefficients and *A* denotes the instantaneous valve areas which are calculated from the mass-spring-damper dynamics. Moreover, ρ signifies fluid density and *U* represents the velocities at which the fluid enters or leaves the control volume. The value of U_i and U_o are calculated by approximating the inlet and outlet valves as adiabatic nozzles. As such, U_i is given as follows:

$$U_i = \begin{cases} \sqrt{2(P_i / \rho_i - P_c / \rho_c)} & \text{if } P_i / P_c \geq \varepsilon_r \\ \sqrt{\gamma R T_c} & \text{if } P_i / P_c \leq \varepsilon_r \end{cases} \qquad 4.4$$

where P_c and P_i are the chamber and inlet pressures respectively and T_c is the chamber temperature. In the equation, ε_r is the critical pressure ratio for working

fluid, γ is its adiabatic exponent and R is its universal gas constant. In a like manner, U_o can be calculated as

$$U_o = \begin{cases} \sqrt{2(P_c/\rho_c - P_o/\rho_o)} & \text{if } P_c/P_o \geq \varepsilon_r \\ \sqrt{\gamma R T_o} & \text{if } P_c/P_o \leq \varepsilon_r \end{cases} \qquad 4.5$$

where P_o and T_o are pressure and temperature respectively on the downstream side of the discharge valve.

To calculate the instantaneous valve areas (i.e., A_i and A_o in equation 4.3), the approach followed by Shu et al (1997) is adopted here. This approach is schematically detailed in Fig 4.1. Dynamically, each valve is simulated by a mass, M_v, supported by a spring of stiffness K_v and a damper of a coefficient C_v. The initial deflection, δ_v, in the valve spring is known along with the lift, L_v. If during calculations the valve motion, z_v is found to fall below the set value for δ_v, the valve would be supported by the seat whose stiffness and damping coefficients are given as K_{seat} and C_{seat} respectively. If z_v is found to fall above the value of $\delta_v + L_v$, the value would be supported by a hard stop whose stiffness and damping coefficients are given as K_{stop} and C_{stop} respectively. Based on this understanding, the following differential equation can be written to describe the valve motion:

$$dz_v^2/d\theta^2 = \left(\frac{1}{M_v\omega^2}\right) \times \begin{cases} f_{v1} & \text{for} \quad \delta_v \leq z_v \leq \delta_v + L_v \\ f_{v2} & \text{for} \quad z_v \leq \delta_v \\ f_{v3} & \text{for} \quad z_v \geq \delta_v + L_v \end{cases} \qquad 4.6$$

where

$$\left.\begin{aligned} f_{v1} &= \Delta P A_v - C_v \omega (dz_v / d\theta) - K_v z_v \\ f_{v2} &= \Delta P A_v - (C_v + C_{seat}) \omega (dz_v / d\theta) - (K_v + K_{seat}) z_v + K_{seat} \delta_v \\ f_{v3} &= \Delta P A_v - (C_v + C_{stop}) \omega (dz_v / d\theta) - (K_v + K_{stop}) z_v + K_{stop} (\delta_v + L_v) \end{aligned}\right\} \quad 4.7$$

where A_v is the valve cross-sectional area and ΔP is equal to $P_i - P_c$ for the inlet valve and $P_c - P_o$ for the discharge valve. The instantaneous value areas (i.e., A_i and A_o), are then calculated using the following formula which is simplified from Tuymer and Machu (2001):

$$A = \sqrt{1/\left((1/0.85 D_s z_v)^2 + 1/A_v^2\right)} \quad 4.8$$

where D_s is the diameter of the valve seat.

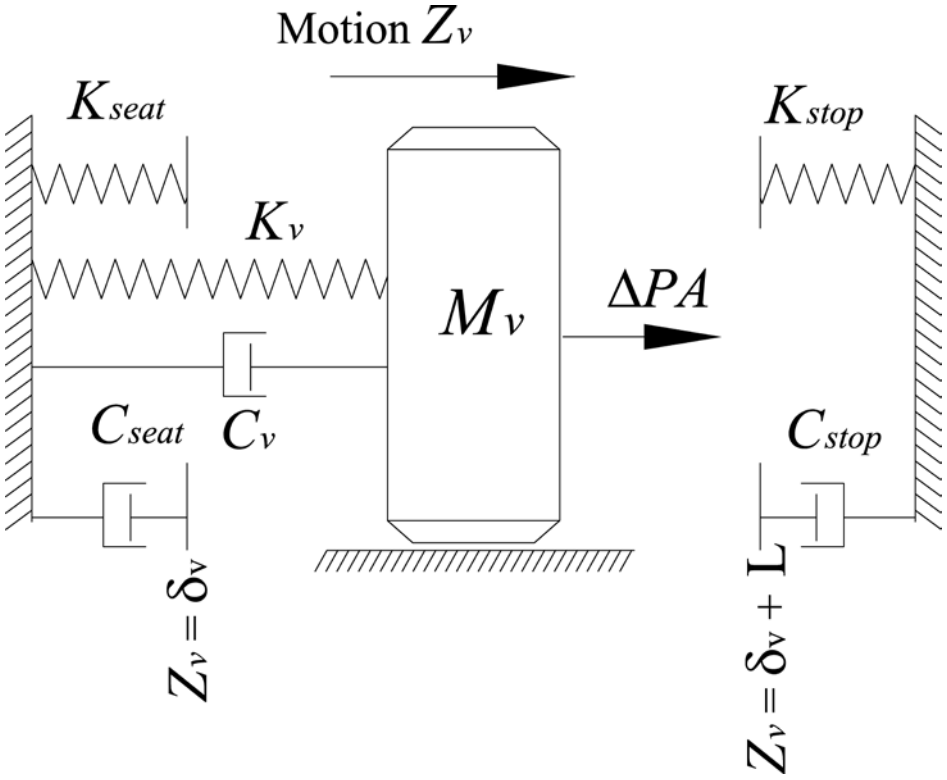

Figure 4.1 The Valve Dynamics

Taking the energy transfer to and from the control volume as an adiabatic process which will result in the following equation;

$$dH_i / d_t - dH_o / dt = d(m_c e_c) / dt + P_c dV_c / dt \qquad 4.9$$

where H_o and H_i are the enthalpies moving in and out of the control volume respectively, and e_c is the specific internal energy available in the control volume. Assuming that the rate at which the temperature varies is small compared to the rates at which other variables change, it will be possible to manipulate Equation 4.9 into the following form:

$$dP_c / d\theta = \left(R\gamma / \omega V_c\right)\left[C_i \rho_i A_i U_i T_i - C_o \rho_o A_o T_c + \left(P_c \omega / R\right) dx / d\theta\right] \qquad 4.10$$

Now the differential equations in equations 4.3, 4.6 and 4.10 may be solved numerically to find instantaneous values for the control pressure, P_c, and density ρ_c at corresponding values for the crank angle θ. At every iteration, the corresponding control volume temperature can be obtained using the equation of state. Also, the temperature T_o, on the downstream side of the discharge valve can be obtained from the adiabatic nozzle process. In such a case, ρ_o can be obtained from the equation of state with P_o and T_o both being known. The instantaneous value of shaft torque, τ_c, which results from the fluid pressure can be expressed as follows:

$$\tau_c = P_c dV_c / d\theta \qquad 4.11$$

The iterative approach proceeds by calculating the thermodynamic model at small intervals in the range $\theta_s \le \theta \le \theta_s + 2\pi$ where θ_s is the crank angle at the start of the

induction stroke as introduced in Chapter 3. The values $P_c(\theta_s)$ and $\rho_c(\theta_s)$, assumed for the chamber pressure and density, respectively, at the start of the cycle are compared to the corresponding values, $P_c(\theta_s + 2\pi)$ and $\rho_c(\theta_s + 2\pi)$, calculated at the end of the cycle using the following dimensionless error expression:

$$e_c = \sqrt{\left(\frac{P_c(\theta_s) - P_c(\theta_s + 2\pi)}{\overline{P}_c}\right)^2 + \left(\frac{\rho_c(\theta_s) - \rho_c(\theta_s + 2\pi)}{\overline{\rho}_c}\right)^2} \qquad 4.12$$

where $\overline{P}_c$ and $\overline{\rho}_c$ are pressure and density values calculated as follows;

$$\overline{P}_c = \frac{P_c(\theta_s) + P_c(\theta_s + 2\pi)}{2} \quad \text{and} \quad \overline{\rho}_c = \frac{\rho_c(\theta_s) + \rho_c(\theta_s + 2\pi)}{2} \qquad 4.13$$

If the outcome of equation 4.12 is larger than a small predefined value, $P_c(\theta_s)$ and $\rho_c(\theta_s)$ are set, respectively, equal to $P_c(\theta_s + 2\pi)$ and $\rho_c(\theta_s + 2\pi)$ to repeat the procedure again over the 2π range of θ. This is iterated until the calculated error, e_c, falls within an acceptable range to reflect the cyclical nature of the thermodynamic process described as has been suggested by Peng et al (2002) and Dagilis et al (2007).

4.3 COMPRESSOR PERFORMANCE

The compressor performance aspects discussed in this chapter are the volumetric efficiency, η_v, the torque steadiness, η_τ, and the cooling susceptibility, η_c.

The volumetric efficiency is defined as the actual volume of the gas (as measured at standard atmospheric conditions) induced into the cylinder in one cycle divided by the volume swept by the piston:

$$\eta_v = V_{in} / V_{swept} \qquad 4.14$$

$$V_{in} = \frac{m_c^{\max} - m_c^{\min}}{P_{atm} / RT_{atm}} \qquad 4.15$$

where $m_c^{\max}$ and $m_c^{\min}$ are, respectively, the maximum and minimum chamber mass calculated during one cycle. In the above equation, P_{atm} and T_{atm}, respectively, denote the air pressure and temperature at standard atmospheric conditions. On the other hand, the torque steadiness is meant to express the spread of the cyclical torque curve around a mean value, τ_m and it can be expressed as follows:

$$\eta_\tau = 1 - \left(\tau_{\max} - \tau_{\mathrm{m}}\right) / \left(\tau_{\max} + \tau_{\mathrm{m}}\right) \qquad 4.16$$

where $\tau_{\max}$ is the peak value on the torque curve. The swept volume and the pressure levels are kept constant during the iterative optimisation process. As such, variations in the mean torque during iterations are expected to be small and higher values for η_τ will more likely reflect reductions in the value of the peak torque to bring it towards the mean value. This will result in a smoother operation, smaller flywheel size and longer lives for various mechanical components.

The cooling susceptibility is meant to measure how efficiently the cooling process is expected to operated. For this purpose, the maximum rate at which the heat is produced during the cycle, $Q_{\max}$, is used to calculate η_c as follows:

$$\eta_c = 1 - \left(Q_{\max} - W_{iso}\right) / \left(Q_{\max} + W_{iso}\right) \qquad 4.17$$

where W_{iso} is the isothermal power calculated for the work cycle. Similar to η_τ, W_{iso} is not likely to vary much amongst iterations, which suggests that higher values for η_c will reflect reductions in the rate at which the heat is produced during the cycle. Reduced values for $Q_{\max}$ will make it possible for the cooling fluid to pick up more of the heat produced during compression stroke. This is in agreement with the conclusions drawn by Catto and Prata (2000) based on their extensive numerical study of the heat transfer phenomenon in reciprocating compressors. The rate at which heat is produced during a cycle is calculated by tracking the internal energy variation, $\Delta m_c e_c$, among successive intervals for the crank angle θ. In this case, $Q_{\max}$ is calculated as follows:

$$Q_{\max} = \omega\left(\Delta m_c e_c / \Delta\theta\right)_{\max} \qquad 4.18$$

where $\Delta\theta$ represents the width of intervals on the θ-axis.

4.4 PERFORMANCE OPTIMISATION

Two kinematic particulars, namely θ_c and θ_d are chosen here as the control parameters which determine the performance of a reciprocating compressor. These respectively, are the crank angles over which the compression stroke occurs and the piston dwells at the end of induction stroke.

Based on the three performance criteria introduced above, the following loss function, f_p is proposed for minimization;

$$f_p\left(\theta_c,\theta_d\right)=w_v\left(1-\eta_v\right)^2+w_c\left(1-\eta_c\right)^2+w_\tau\left(1-\eta_\tau\right)^2 \qquad 4.19$$

where w_v, w_c and w_τ are positive weighting values assigned subjectively to reflect the importance of each performance criterion for a particular design. The functional form presented for f_p in equation 4.19 highlights its dependence on the design parameters, θ_c and θ_d.

The approach of Simultaneous Perturbation Stochastic Approximation (SPSA) is adopted here for the second level optimisation procedure. SPSA is efficient and suited for such an intricate optimisation application as abundantly explained in literature, e.g., the excellent paper by Spall (1992) and interesting application presented by Kothandaraman and Rotea (2005). In accordance with this technique, the updated values of the design parameters are calculated at the end of iteration step number i as follows:

$$\left.\begin{aligned}\theta_c^{i+1}&=\theta_c^i-\delta\theta_c^i\\ \theta_d^{i+1}&=\theta_d^i-\delta\theta_d^i\end{aligned}\right\} \qquad 4.20$$

where $\delta\theta_c^i$ and $\delta\theta_d^i$ are the connection values which are calculated as follows:

$$\delta\theta_c^i=a_i\left[\,f_p\left(\theta_c^i+C_i\Delta_c^i,\theta_d^i+C_i\Delta_d^i\right)-f_p\left(\theta_c^i-C_i\Delta_c^i,\theta_d^i-C_i\Delta_d^i\right)\right]/\left(2C_i\Delta_c^i\right)$$

$$\delta\theta_d^i=a_i\left[\,f_p\left(\theta_c^i+C_i\Delta_c^i,\theta_d^i+C_i\Delta_d^i\right)-f_p\left(\theta_c^i-C_i\Delta_c^i,\theta_d^i-C_i\Delta_d^i\right)\right]/\left(2C_i\Delta_d^i\right) \qquad 4.21$$

where Δ_c^i and Δ_d^i are randomly assigned the values of either +1 or -1 as generated, at every iteration, by a binary Bernoulli distribution. The parameters a_i and C_i are the sequence gains which are calculated at iteration number i as follows:

$$\left.\begin{aligned} a_i &= a/\left(B+i\right)^{0.602} \\ C_i &= c/\left(i\right)^{0.101} \end{aligned}\right\} \qquad 4.22$$

Spall (1992) points out the guidelines which may be followed to select numerical values for the constants, a and c, in equation 4.20. For the work presented here, which features a low-noise application, c has been equal to 0.0055 and a is set equal to 0.35. The value of B is calculated as $N_{\max}/10$ where $N_{\max}$ is the maximum allowable number of iterations set at the start of the procedure. The limits imposed on the values of θ_c (i.e. $\theta_{c\min}$ and $\theta_{c\max}$) and θ_d (i.e. $\theta_{d\min}$ and $\theta_{d\max}$) are incorporated in the procedure as follows:

$$\theta_c^{i+1} = \begin{cases} \theta_{c\max} \; if \; \theta_c^{i+1} \geq \theta_{c\max} \\ \theta_{c\min} \; if \; \theta_c^{i+1} \leq \theta_{c\min} \end{cases} \qquad 4.23$$

and

$$\theta_d^{i+1} = \begin{cases} \theta_{d\max} \; if \; \theta_d^{i+1} \geq \theta_{d\max} \\ \theta_{d\min} \; if \; \theta_d^{i+1} \leq \theta_{d\min} \end{cases} \qquad 4.24$$

A case study is presented in the next section to detail how the models presented in this paper are utilized for compressor design.

CASE STUDY

The computer implementation of the hybrid two-level approach is detailed by the flow chart given in Figure 4.2.

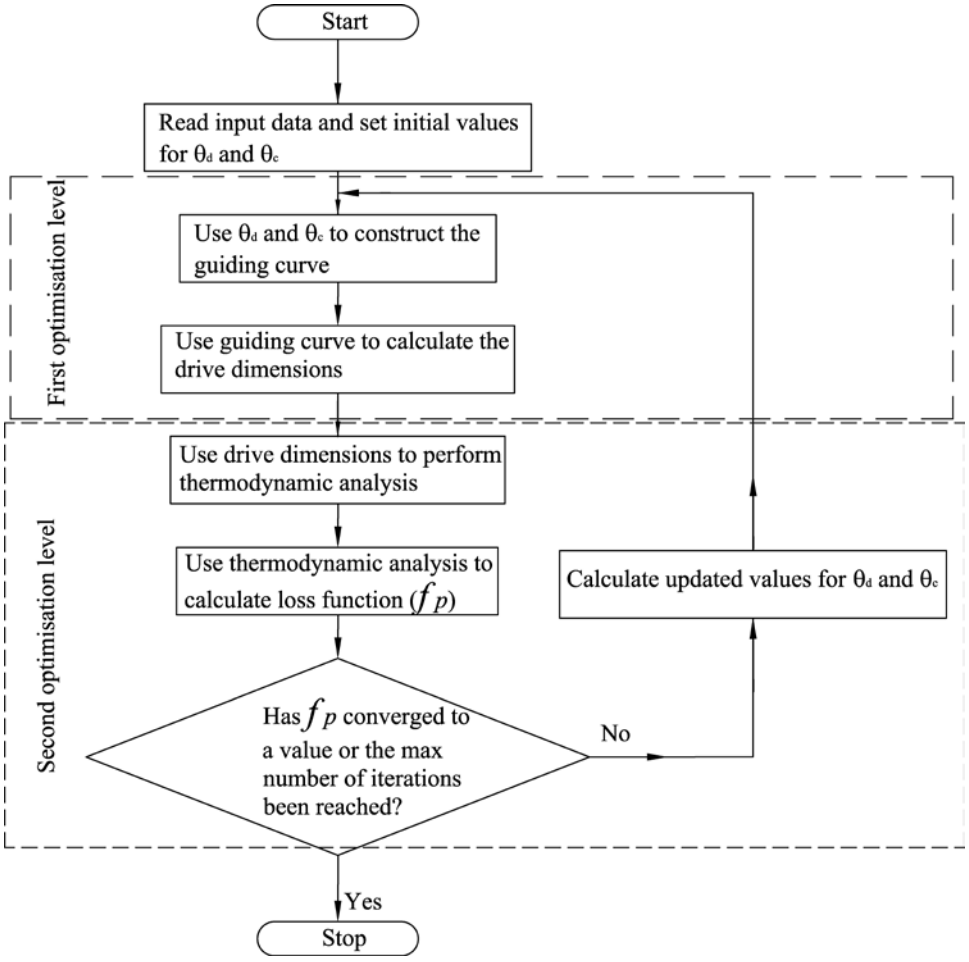

Figure 4.2 Flowchart of the Optimisation procedure

The procedure starts with initial values assigned to the two design parameters, θ_c and θ_d. This is then followed by a gradient-based first level optimisation procedure, which is detailed in Chapter 3, undertaken to calculate dimensions for mechanism which realizes these two design parameters. The stochastic second level optimisation procedure is then undertaken to use the resulting mechanism for the thermodynamic

analysis to calculate the performance aspects referred to above together with the loss function. The values for θ_c and θ_d are then modified to use again in the first model optimisation procedure. To prove the validity of the approach presented here, it was applied to a numerical example with the following particulars:

Crank speed = 800 rev/min Bore diameter = 120 mm P_i = 1 bar

P_o = 6 bar T_i = 20 ^{o}C inlet and outlet valve diameters respectively are 50 mm and 40 mm. The dynamical properties for the value were set similar to the values used by Haping (2005). The maximum value for θ_c was set equal to 220 ^{o} and its minimum value was 180 ^{o}. The maximum value for θ_d was set equal to 40 ^{o}C and its minimum value was 0 ^{o}C. The constant stroke length was 100 mm and the initial values for θ_c and θ_d were set equal to 180 ^{o} and 0 ^{o} respectively. These settings correspond to the following drive dimensions which have been defined in Chapter 3:

θ_s = 0.90 ^{o} φ_s = -179.12 ^{o} μ_s = -1.2 ^{o}

r_{c1} = 31.4 mm r_{cn} = 18.57 mm l_a = 150.0 mm

The best values for θ_c and θ_d were found to be 205.08 ^{o} and 7.37 ^{o} respectively; and the optimised drive has the following dimensions;

θ_s = -24.08 ^{o} φ_s = -201.14 ^{o} μ_s = 8.66 ^{o}

r_{c1} = 26.71 mm r_{cn} = 33.24 mm l_a = 146.42 mm

A scaled rendering of this drive is shown in Figure 4.3.

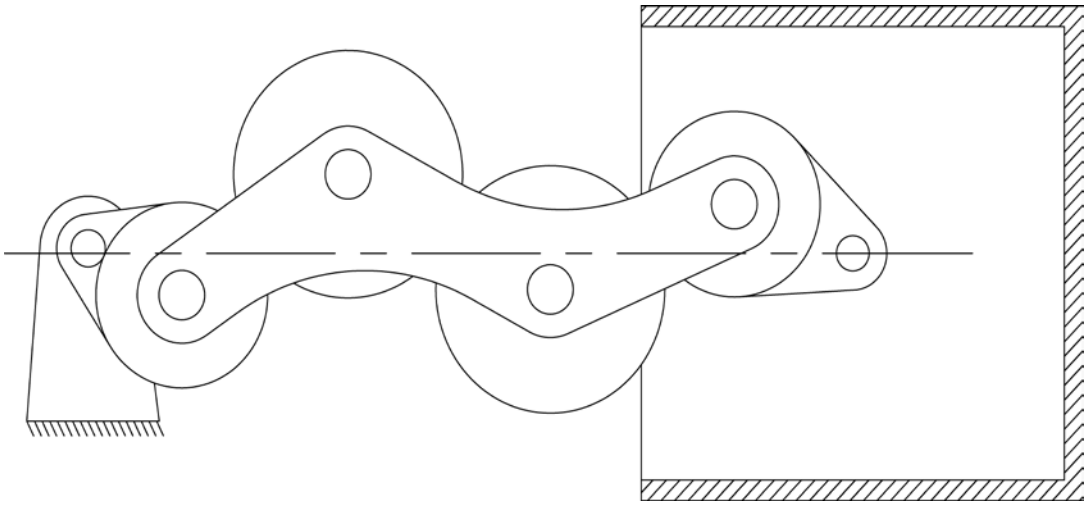

Figure 4.3 A rendering for the resulting compressor drive

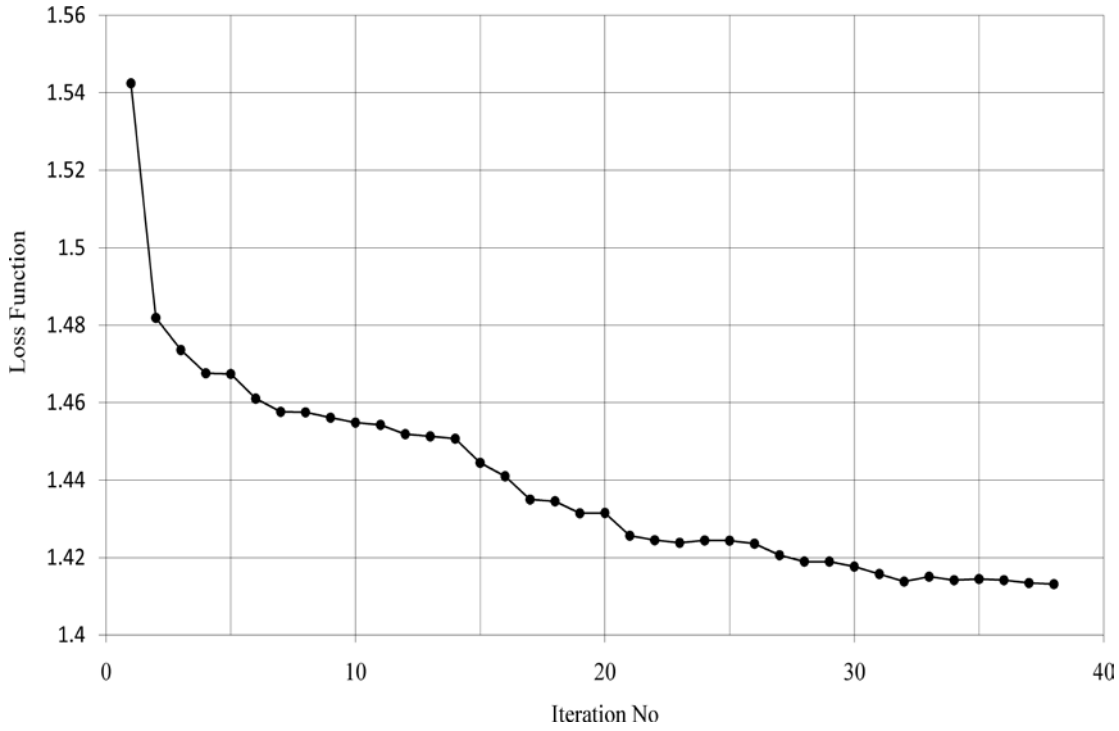

Figure 4.4 Reduction of the loss function with iterations

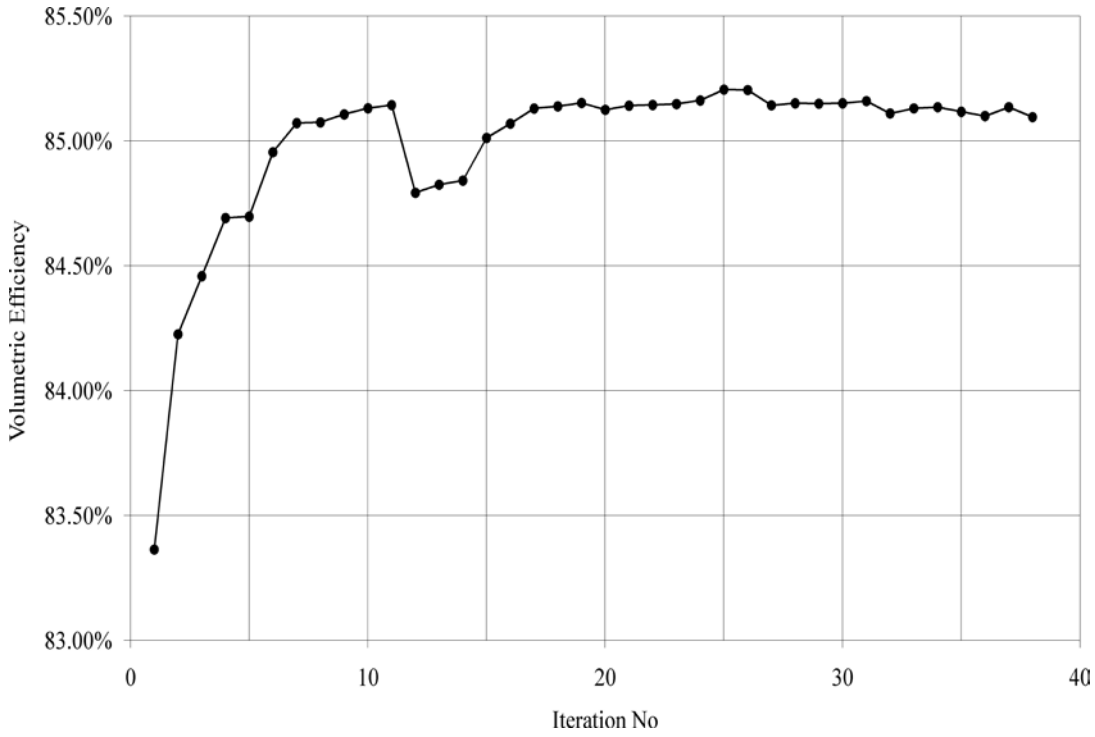

Figure 4.5 Improvement of volumetric efficiency with iterations

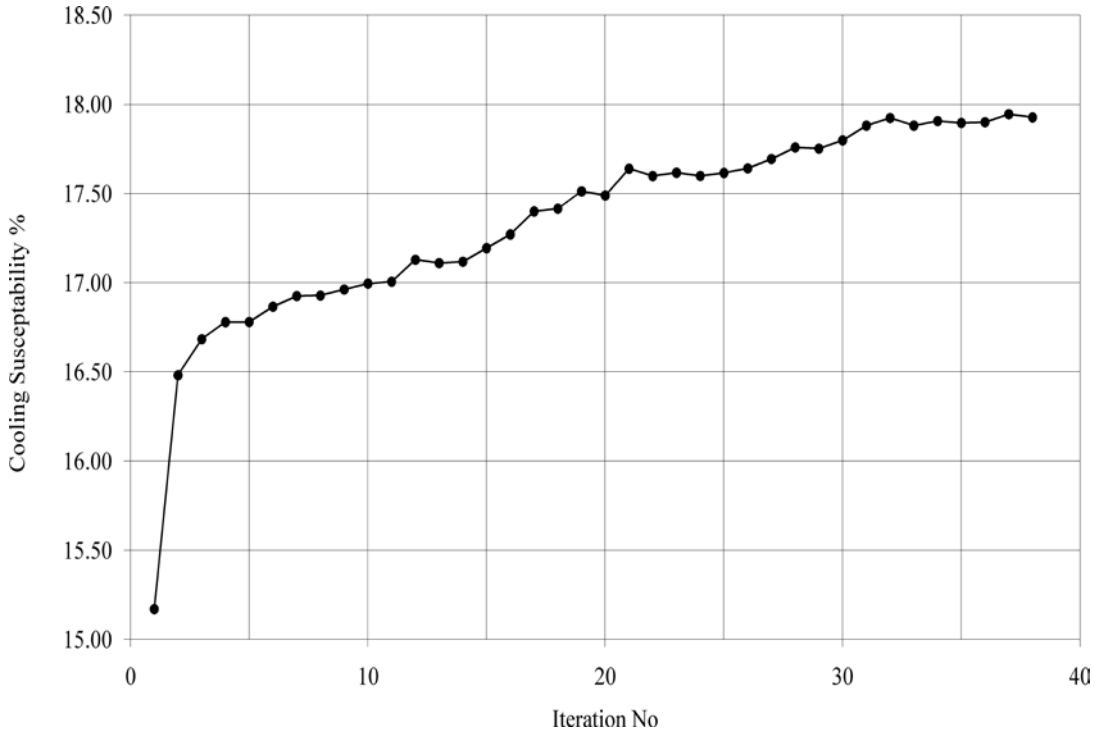

Figure 4.6 Improvement of cooling susceptibility with iterations

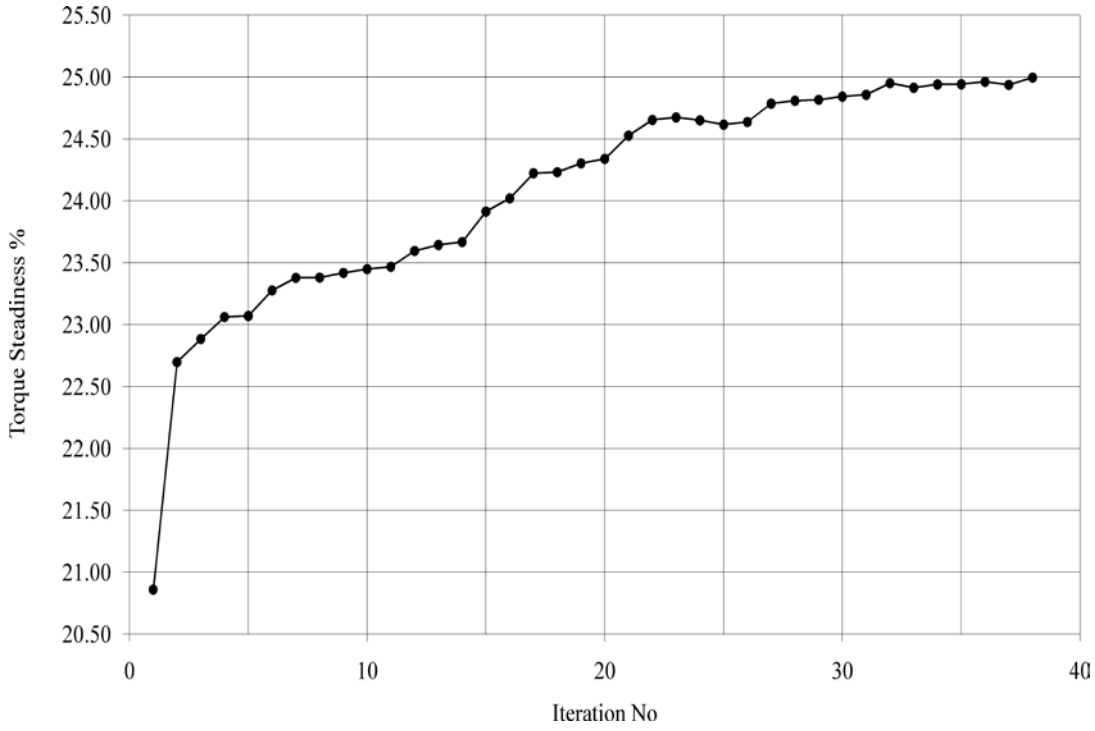

Figure 4.7 Improvement of torque steadiness with iterations

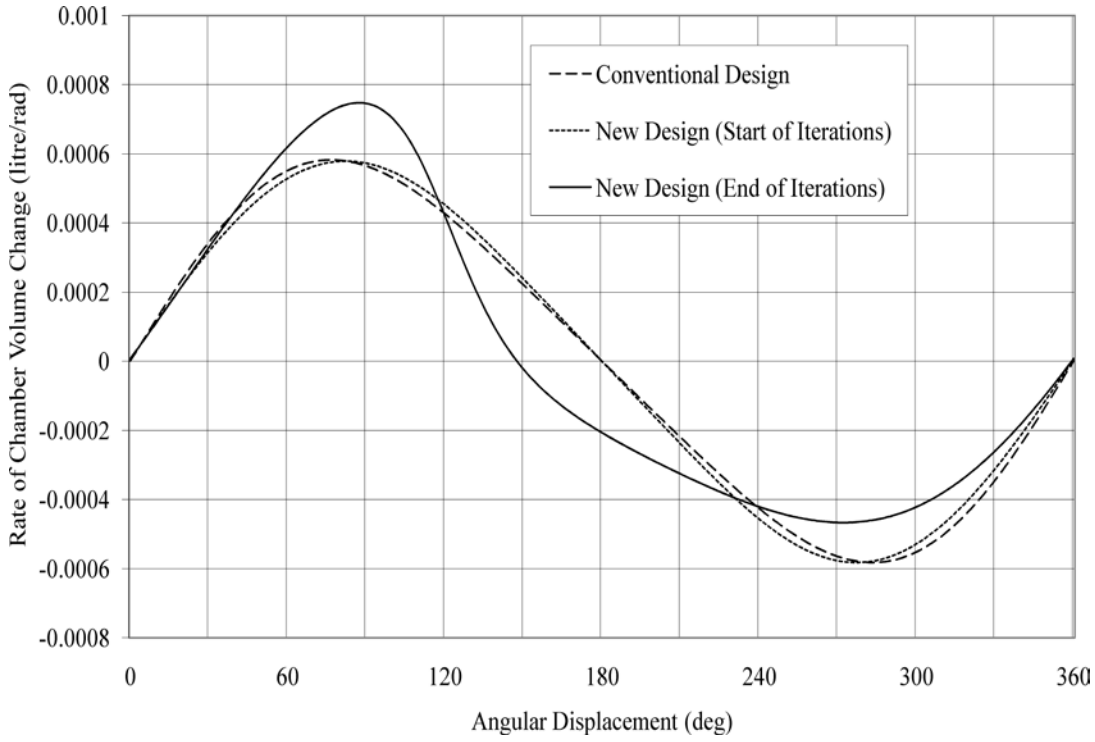

Figure 4.8 The volume-angle gradient

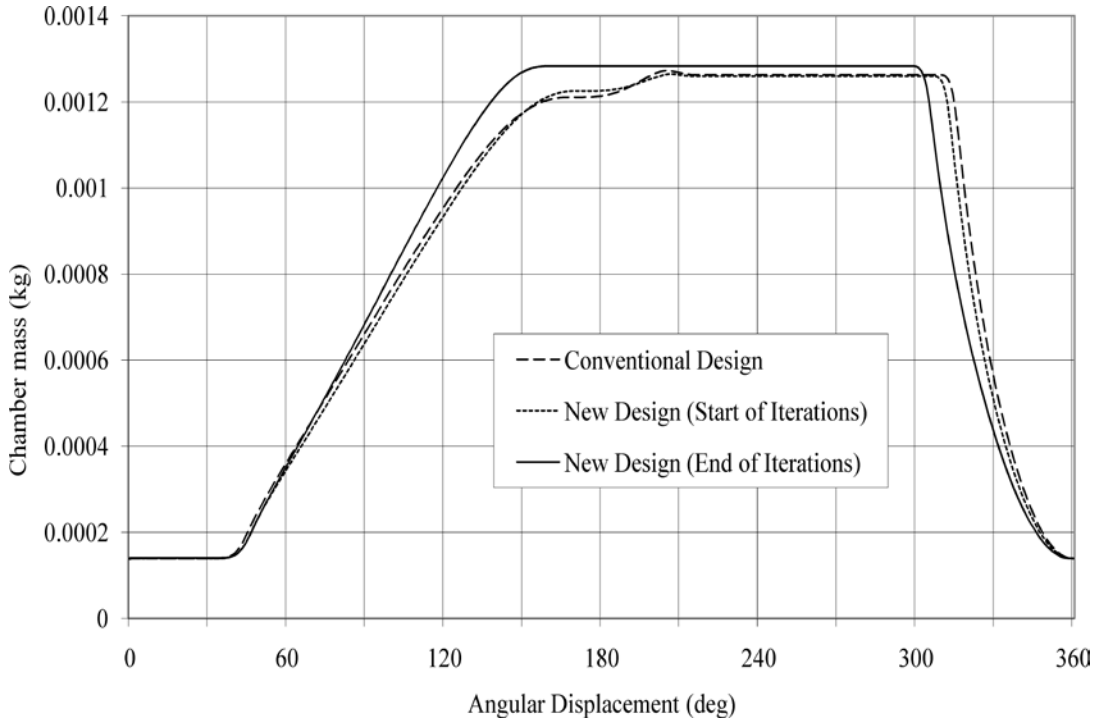

Figure 4.9 Chamber mass vs. crank angular displacement

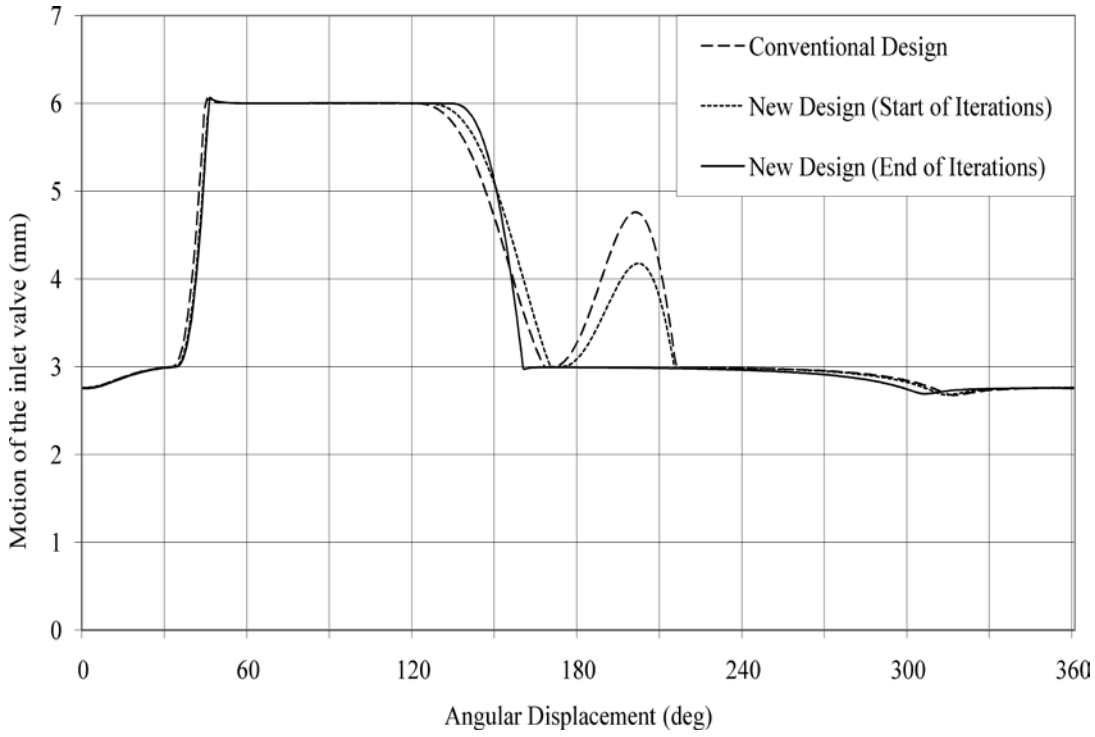

Figure 4.10 Inlet valve motion vs. crank angular displacement

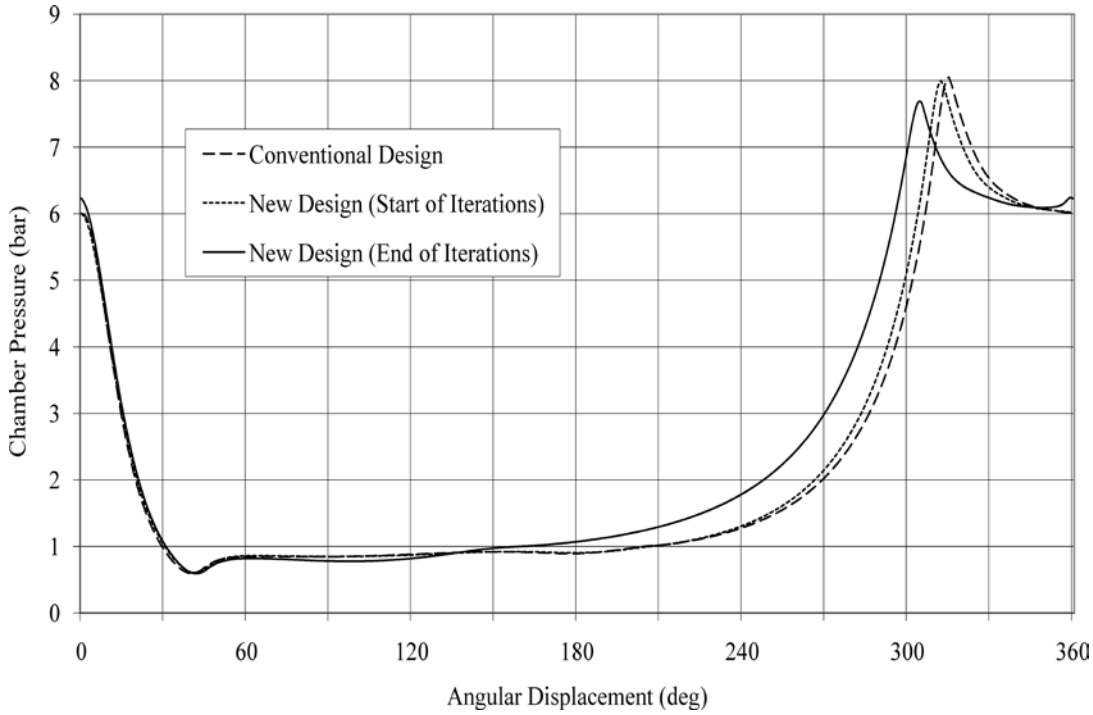

Figure 4.11 Chamber pressure vs. angular displacement

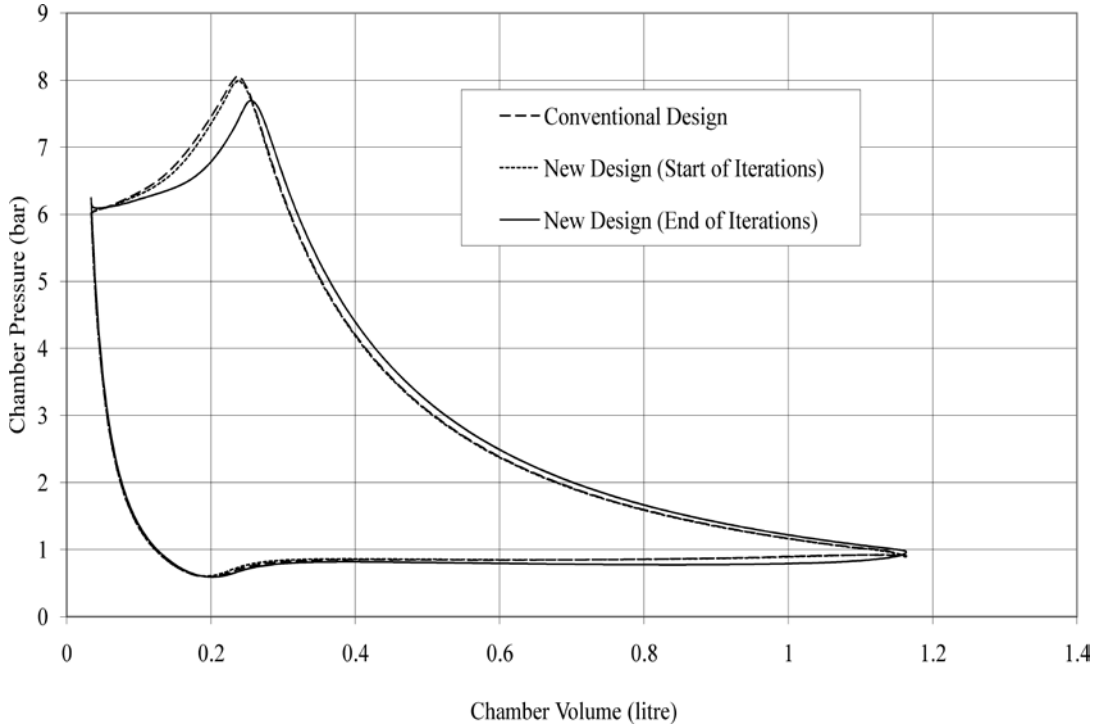

Figure 4.12 The PV diagram

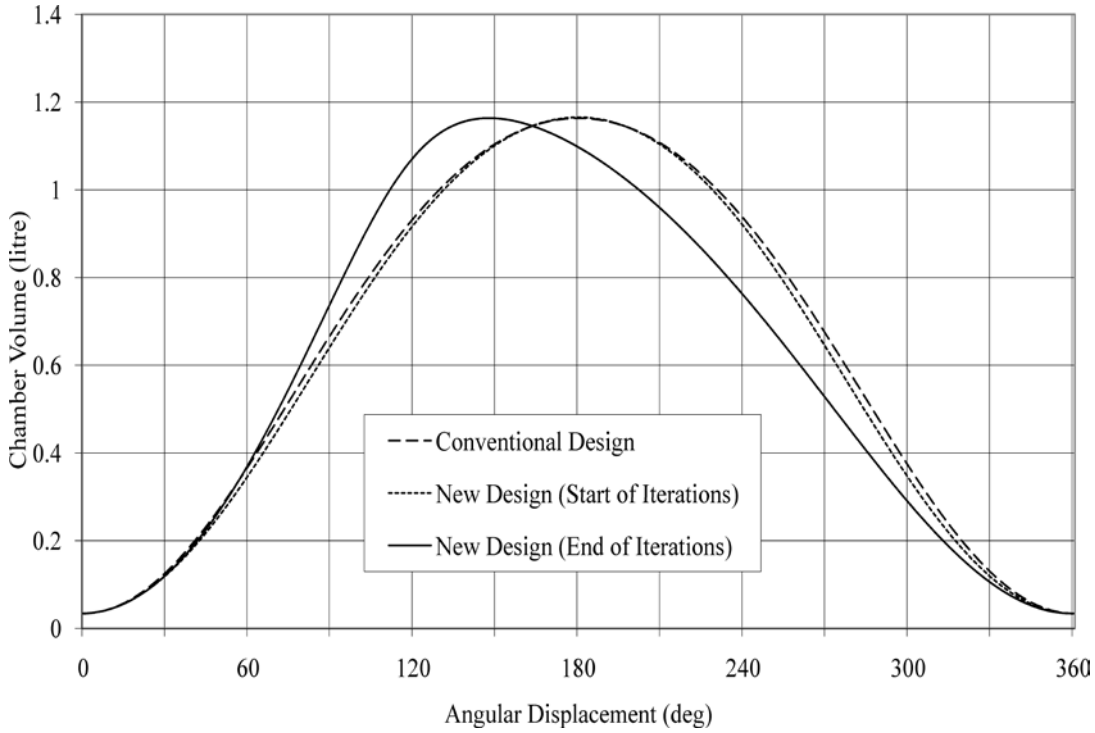

Figure 4.13 Chamber vs. the crank angular displacement

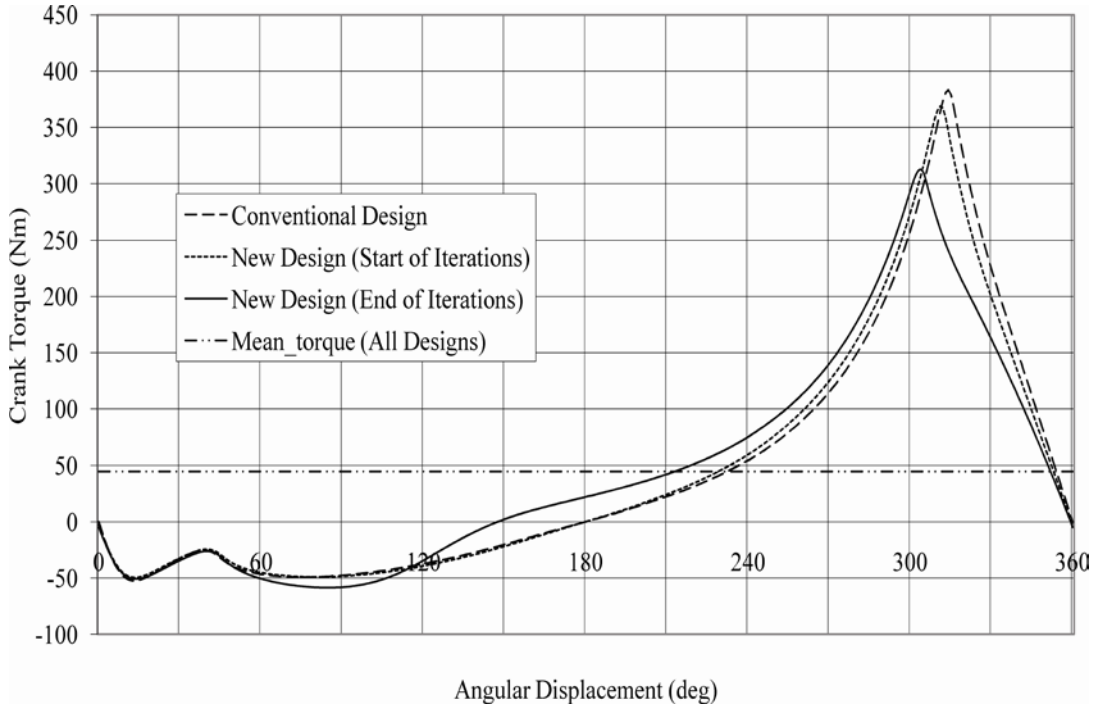

Figure 4.14 Crank torque (due to gas pressure) vs. the crank angular displacement

RESULTS AND DISCUSSIONS:

Figures 4.4, 4.5, 4.6 and 4.7 depict the values obtained for the loss function and performance criteria during the optimisation process. The improvement achieved should be regarded in reference to Figure 4.8 which compares the rate at which the chamber volume changes (i.e. $dV_c / d\theta$) obtained for each of the optimised compressor. All are made to have the same stroke, speed, bore diameter and clearance volume. As shown in the figure, the volume of the optimised compressor increases at a faster rate up to midway through the induction stroke, but then the piston slows down before the end of induction. This speed reduction leads to a short dwell at the end of the stroke. The dwell provides time for the air to flow as evident by Figure 4.9. This figure depicts the mass of air in the chamber against the crank angular displacement. Figure 4.8 shows that at the start of the compression stroke, the piston of the optimised compressor speeds up in order for the chamber volume to decrease at a higher rate when the pressure is still too low. This creates an early pressure rise to suppress the inlet valve bounce as shown in Figure 4.10, which features the inlet valve motion for the three compressors indicated. For the three cases, the valve had the same values for the masses, spring constants and damping coefficients. Figure 4.10 suggests more stable dynamic characteristics for the optimised compressor valve. Interestingly, the valve bounce may allow for more mass to flow into the chamber of the conventional compressor as indicated in Figure 4.9 by a jump in the relevant curve. However, this contributes to noise and reduced reliability.

Figure 4.8 also suggests that during the compression stroke as the pressure builds up, the piston slows down. This reduces the rate at which the pressure and, consequently, the heat are generated and allows the cooling system more time for heat removal.

Similarly, the outlet valve is allowed more time to react when the pressure has reached the desired discharge valve. As such, the maximum pressure in the cylinder is expected to be less than the maximum pressure values exhibited by the other two compressors shown in Figure 4.8. This favourable behaviour is shown in Figure 4.11 which depicts the pressure-angle profile in one cycle of the compressor operation. The PV-diagram which is shown in Figure 4.12 also asserts the same notion. This volumetric behaviour, when combined with the fact that the pressure stroke does occupy a larger crank angle than the induction stroke (as shown in Figure 4.13), suggests that the torque will be better spread over the cycle, which will reduce the value of maximum torque required at the crank. This is evident in Figure 4.14 which offers a visual representation of the crank torque profile. The reduction in the value of the maximum torque combined and the better spread profile leads to better reliability, longer service life for various components, smaller flywheel size, low noise and vibration characteristics.

The next chapter presents thesis conclusions and recommendations for future work.

Chapter 5

Conclusions and Recommendations for Future Work

This thesis discusses the utilisation of the geared five-bar slider-crank mechanism to drive positive displacement machines. This geared mechanism is able to produce favourable stroke characteristics which will not only improve the thermodynamic performance of the positive displacement machine, but will also reduce maximum crankshaft torque and flywheel size. This is expected to increase the service life of machine components and reduce unfavourable dynamical effects.

The thesis presented a numerical position analysis for the mechanism studied which is based on the concepts of differential kinematics where a Jacobian matrix has been obtained and utilised to solve a set of simple first order differential equations using the Euler method. Insights into the kinematic equations revealed that the geared five-bar slider-crank mechanism may be classified into Type-1 and Type-2 mechanisms based on which link, other than the crank, is allowed to perform full rotations in one cycle of the mechanism motion. The results of the kinematic analysis have been utilised in a gradient-based optimisation technique implemented to design the mechanism dimensions which would constrain the piston to follow a given

trajectory. This optimisation model features the method of Levengberg-Marquardt which is robust and could be made to proceed slowly during the iterative process in order for the solution points not to be missed.

Case studies have been presented to prove the validity of the synthesis model and to investigate the aspects of the obtained solutions. The weighting values, assigned to various points on the desired trajectory, have been found to influence the outcome of the obtained results in such a way that may reduce the functionality of the mechanism. This suggests that the designer may have to carefully adjust these weights upon inspecting the obtained results.

To put it all together, a case study was presented in Chapter 4 in which a geared five-bar slider-crank mechanism was optimised to improve the workings of a reciprocating compressor. This application features the need to optimise the piston trajectory, which in return requires optimisation of the mechanism dimensions to realise this trajectory. A two-level optimisation problem which was solved in this thesis by employing two different optimisation techniques. Whilst, a gradient-based formulation, as pointed out above, has been used for the mechanism synthesis, a stochastic-based technique was utilised for the trajectory optimisation. This was dictated by the degree of difficulty present in the trajectory optimisation problem. The approach featured in the thesis requires calculations of the thermodynamic performance of the reciprocating compressors. A task which was achieved through the utilisation of a differential-based thermodynamic model.

The results obtained for the compressor case study presented in the thesis are promising where a few percentage points improvements have been achieved for the selected performance indices of the compressor.

For future work, it is recommended that a dynamic study be conducted on the mechanism in question to investigate the effects of various forces on the performance and propose means to ensure smooth running for the mechanism. Also, it is recommended that based on the results of this thesis and future investigations, a prototype reciprocating compressor be manufactured and employed in a laboratory-based testing program to assert the results of theoretical studies and propose further developmental work.

References

1. Antoniou A., and Lu W. S., 2007, “Practical optimization: Algorithms and Engineering Applications”, Springer Science + Business Media, LLC, 233 Springer Street, New York, NY 10013, USA, pp. 272-274.

2. Buskiewicz, J., 2006, “A Method of Optimization of Solving a Kinematic Problem with the use of Structural Analysis Algorithm (SAM)”, Mechanism and Machine Theory, Vol. 41, pp. 823-837.

3. Bresland, C. N., 2001, U. S. Patent No.: US 6,273,052 B1, August 14.

4. Cabrera, J. A., Simon, A., and Prado, M., 2002, “Optimal Synthesis of Mechanism with Genetic Algorithms”, Mechanism and Machine Theory, Vol. 37, pp.1165-1177.

5. Catto, A. G., and Prata A., T., 2000, “A Numerical Study of Instantaneous Heat Transfer During Compression and Expansion in Piston-Cylinder Geometry”, Numerical Heat Transfer, Part A, Vol. 38, pp. 281-303.

6. Cho, J. R., and Moon, S., J., 2005, “A Numerical Analysis of the Interaction between the Piston Oil Film and the Component deformation in a Reciprocating Compressor”, Tribology International, Vol. 38, pp. 459-468.

7. Cossalter, V., Doria, A., Pasini, M and Scattolo, C., 1992, “A Simple Numerical Appraoch for Optimum Synthesis of a Class of Planar Mechanisms”, Mech. Mach. Theory, Vol.27 (3), pp.357-366.

8. Dagilis, V., Vaitkus, L., and Kirejchich, D., 2006, “Slider-Link Driven Compressor (I). Mathematical Model”, -Mechanika. -Kaunas: Technologija, No. 6(62), pp. 25-31.

9. Dagilis, V., Vaitkus, L., and Kirejchich, D., 2007, “Slider-Link Driven Compressor (II). Simulation Results”, -Mechanika. -Kaunas: Technologija, No. 1(63), pp. 50-57.

10. Dagilis, V., Vaitkus, L., and Kirejchich, D., 2007, “Slider-Link Driven Compressor (III). Optimization”, -Mechanika. -Kaunas: Technologija, No. 3(63), pp. 46-50.

11. Deb, K., Tiwari, S., 2005, “Multi-Object Optimization of a Leg Mechanism using Genetic Algorithms”, Engineering Optimization, Vol. 37, No. 4, 325-350.

12. Dooner, D. B., 2001, “Function Generation Utilizing and Eight-Link Mechanism and Optimized Non-Circular Gear Elements with Application to Automotive Steering”, Proc. Instn. Mech. Engrs., Vol.215, Part C, pp. 847-857.

13. Etman, L. F., P., Campen, D., H., V., and Schoofs A., J., G., 1998, "Design Optimization of Multibody System by Sequential Approximation", Multibody System Dynamics 2: , pp. 393-415.

14. Estupinan, E. A., and Santos, I. F., 2007, "dynamic Modelling of Hermetic Reciprocating Compressors, Combining Multibody Dynamics. Finite Elements Method and Fluid Film Lubrication", Int. J. Mechanics, Vol. 1(4), pp.36-43

15. Feng, B., Morita, N., and Torii, T., 2002, "A New Optimization Method for Dynamic Design of Planar Linkage with Clearances at Joints – Optimizing the Mass Distribution of Links to Reduce the Change of Joint Forces", ASME, Vol. 124, pp. 68-72.

16. Gabrielle, G. A., 1993, "Optimization in Mechanisms, in Erdman, A. (Ed.). *Modern Kinematics in the Last Forty Years*", John Wiley & Son Inc. New York.

17. Gatti, G., and Mundo, D., 2007, "Optimal Synthesis of Six-Bar Cammed linkages for Exact Rigid-Body Guidance", Mechanism and Machine Theory, Vol. 42, pp. 1069-1081.

18. Hansen, J. M., 2002, "Synthesis of Mechanism Using Time-Varying Dimensions", Multibody System Dynamics, Vol. 7, pp. 126-144.

19. Haping, R. A., 2005, "Flow and plate Motion in Compressor Valve," Doctoral Thesis, University of Twente, Enschede, The Netherlands.

20. Haung, C., and Roth, B., 1993, "Dimensional Synthesis of Closed-Loop to Match Force and Positions Specifications", ASME, VOl. 115, pp. 195-198.

21. Jensen, O. F., and Hansen, J. M., 2006, "Dimensional Synthesis of Spatial Mechanism and the Problem of Non-Assembly", Multibody System Dynamics, Vol. 15, pp 107-133.

22. Kothandaraman, G., and Rotea, M., A., 2005, "Simultaneous-Perturbation-Stochastic-Approximation Algorithm for Parachute Parameter Estimation", Journal of Aircraft, Vol. 42, No.5, pp. 1229-1235.

23. Lekic, U. and Kok, J. B. W., 2008, "Heat Flows in Piston Compressors", Proceedings of the 5th European Thermal Sciences Conference, The Netherlands.

24. Lio, M. D., Cossalter, V., and Lot, R., 2000, "On the Use of Natural Coordinates in Optimal Synthesis of Mechanisms", Mechanism and Machine Theory, Vol. 35, pp. 1367-1389.

25. Liu, Y., and McPhee, J., 2005, "Automated Type Synthesis of Planar Mechanism Using Numeric Optimization with Genetic Algorithms", Journal of Mechanical Design, ASME, Vol. 127, pp. 910-915.

26. Martin, P. J., Russell, K., and Sodhi, R., S., 2007, "On Mechanism Design Optimization for Motion Generation", Mechanism and Machine Theory, Vol. 42, 1251-1263.

27. Michlin, Y., and Myunster, V., 1996, “Determination of Power Losses in Gear Transmission With Rolling and Sliding Friction Incorporated”, Mech. Mach. Theory, Vol. 31, pp831-838.

28. Minaar, R. J., Tortorelli, D. A. and Snyman, J. A., 2001, “On Nonassembly in the Optimal Dimensional Synthesis of Planar Mechanisms”, Structural Multidisc Optimization, Vol. 21, pp. 345-354.

29. Mundo, D., and Yan, H. S., 2007, “kinematic Optimization of Ball-Screw Transmission Mechanisms”, Mechanism and Machine Theory, Vol. 42, pp. 34-47.

30. Nieter, J. J. and Singh, R., 1984, “A Computer Simulation Study of Compressor Tuning Phenomena”, J. Sound and Vibration, Vol. 97 (3), pp.475-488.

31. Nokelby, S. B., and Podhorodeski R., P., 2001, “Optimization-Based Synthesis of Grashof Geared Five-Bar Mechanisms”, Journal of Mechanical Design, ASME, Vol. 123, 529-534.

32. Peng, X., Xing, Z., Li, L., and Shu, P., 2002, “Thermodynamic Analysis of the Rotary Tooth Compressor”, Journal of Power and Energy, Proceedings Institution of Mechanical Engineers, Part A, Vol. 216, pp. 321-327.

33. Rigola, J., 2002, “Numerical Simulation and Experimental Validation of Hermetic Reciprocating Compressors. Integeration in Vapour Compression Refrigerating Systems, “Doctoral Thesis, Polytechnique University of Catalonia, Catalonia, Spain.

34. Rigola, J., Perez-Segarra, C. D., Raush, G., and Oliva A., 2004, ”Detailed Experimental Validation of the Thermal and Fluid Dynamic Behaviour of Hermetic Reciprocating Compressors” HVAC&R Research, Vol. 10 No. 3, pp. 291-306.

35. Rovaris, J. B., and Deschamps, C., J., 2006, “Large Eddy Simulation Applied to Reciprocating Compressors”, Journal of the Braz. Soc. Of Mech. Sci. & Eng., Vol. XXVIII, No. 2, pp. 208-215.

36. Sancibrain, R., Viadero F., Garcia, P., and Fernandez, A., 2004, “Gradient-Based Optimization of Path Synthesis Problems in Planar Mechanisms”, Mechanism and Machine Theory, Vol. 39, pp. 839-856.

37. Shiakolas, P. S., Koladiya D., and Kebrle, J., 2005, “On the Optimum Synthesis of Six-Bar Linkages using Differential Evolution and the Geometric Centroid of Precision Position Technique”, Mechanism and Machine Theory, Vol. 40, pp. 319-335.

38. Shu, J-J., Burrows, C. R., and Edge, K. A., 1997, “Pressure Pulsations in Reciprocating Pump Piping Systems Part 1: Modelling”, Proceeding Institution of Mechanical Engineers, Vol. 211 Part I, pp. 229-236.

39. Smaili, A. A., Diab, N. A., and Atallah N. A., 2005, “Optimum Synthesis of Mechanism using Tabu-Gradient Search Algorithm”, Journal of Mechanical Design, ASME, Vol. 127, pp. 917-923.

40. Smaili, A., and Diab, N., 2007, “A New Approach to Shape optimization for Closed Path Synthesis of Planar Mechanisms”, Journal of Mechanical Design, ASME, Vol. 129, pp. 941-948.

41. Spall, J. C., 1992, “Multivariate Stochastic Approximation Using a Simultaneous Perturbation Gradient Approximation”, IEEE Transactions on Automatic Control, Vol. 37 No. 3, pp. 332-340.

42. Stouffs, P., Tazerout, M., and Wauters, P., 2001, “Thermodynamic Analysis of Reciprocating Compressors”, International Journal of Thermal Science, Vol. 40, pp. 52-66.

43. Suchora, D.H. and Savage, M., 1974, “Geared Five bar Crank Mechanism – Part I: Analysis” an ASME Publication 74-DET-40.

44. Suchora, D. H. and Savage, M., 1974, “Geared Five bar Crank Mechanism – Part II: Design” an ASME Publication 74-DET-41.

45. Sultan I. A., 2002, “Kinematic Modelling of a New Gear-Coupled Mechanism”, 4th International Conference On Modelling and Simulation, Victoria University, Melbourne, Australia, November 11-13, pp. 356-362.

46. Sultan I. A., 2005, “The Limacon of Pascal: Mechanical Generation and Utilisation for Fluid Processing”, Proc. Inst. Mech. Engrs., Vol 219(8) Part C: J. Mechanical Engineering Science, pp.813-822.

47. Sultan I. A., 2006, “Profiling Rotors for Limacon-to-Limacon Compression-Expansion Machines”, ASME J. Mech. Des. 128, pp787-793.

48. Tai, K., Cui, G. Y., and Ray, T., 2002, “Design Synthesis of Path Generating Compliant Mechanism by Evolutionary Optimization of Topology and Shape” ASME, Vol. 124, 492-499.

49. Teng, C. -P., and Angeles, J., 2005, “An optimality Criterion for the Structural Optimization of Machine Elements”, Journal of Mechanical Design, ASME, Vol.127, pp. 415-422.

50. Tuymer, W. J. and Machu, E. H., 2001, “Compressor Valves, in Hanlon. P. C. (Ed.), Compressor Handbook”, The McGraw-Hill Companies, Inc. New York.

51. Yu, Q., and Lee, H., P., 1996, “Curvature Optimization of a Cam Mechanism with a Translating Flat-Faced Follower”, Journal of Mechanical Design, Transaction of the ASME, Vol. 118, pp. 446-449.

52. Zhang, X., Zhou, Ji., Ye, Y., 2000, “Optimal Mechanism Design Using Interior-Point Methods”, Mechanism and Machine Theory, Vol. 35, pp. 83-98.

Appendix A

A1. The Cosine Function

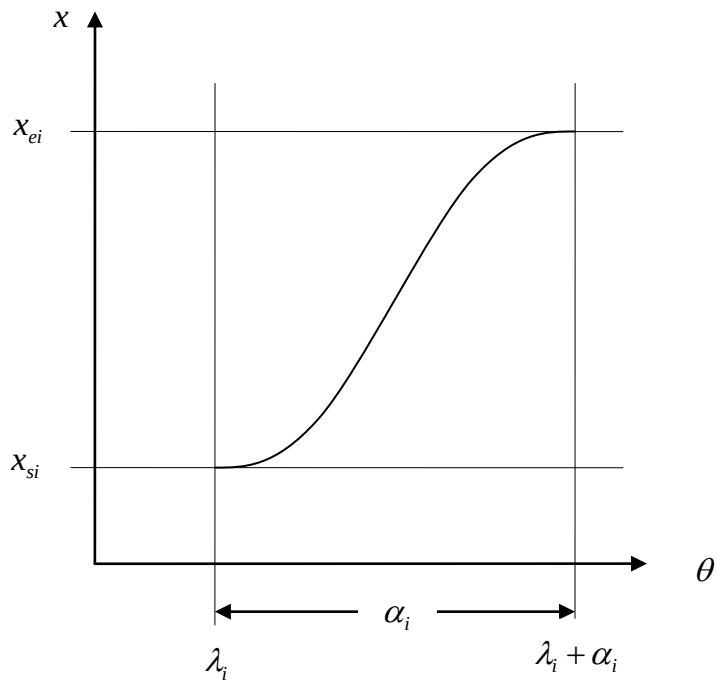

Figure A.1. Curve Section Number i

Reference is made to Fig A.1. The figure shows section number i of the synthetic curve which is used to define the desired piston motion. The parameters of the curve section are given as follow;

λ_i = start of the curve section number i

α_i = width of the curve

x_{si} = x-value at the start

x_{ei} = x-value at the end

The curve equation is given as follows:

$$x_i(\theta) = x_{oi} + a_i\, Cos\,(n_i\theta + \phi_i)$$

where x_{oi}, a_i, n_i and ϕ_i are constants to be calculated from the initial and final conditions.

$$x_i(\lambda_i) = x_{si}$$

$$\frac{dx_i}{d\theta}(\lambda_i) = 0$$

$$x_i(\lambda_i + \alpha_i) = x_{ei}$$

$$\frac{dx_i}{d\theta}(\lambda_i + \alpha_i) = 0$$

From the initial and final conditions it may be shown that the value of the curve constants are given as follows:

$$x_{oi} = \frac{1}{2}(x_{si} + x_{ei})$$

$$a_i = \frac{1}{2}(x_{si} - x_{ei})$$

$$n_i = \frac{\pi}{\alpha_i}$$

$$\phi_i = -\frac{\pi\lambda_i}{\alpha_i}$$

A2. **Polynomial Splines**

If instead of the cosine function given in A.1, a 5th degree polynomial spline is to be adopted for the curve section, its relationship may be given as follows;

$$x_i(\theta) = x_{si} + a_i(\theta - \lambda_i)^2 + b_i(\theta - \lambda_i)^4 + c_i(\theta - \lambda_i)^5$$

This form fulfils three initial conditions, being: $x_i(\lambda_i) = x_{si}$, $\frac{dx_i}{d\theta}(\lambda_i) = 0$ and $\frac{d^2x_i}{d\theta^2}(\lambda_i) = 0$. The three coefficients a_i, b_i and c_i can be calculated from three end conditions given as follows;

$$x_i(\lambda_i + \alpha_i) = x_{ei}$$

$$\frac{dx_i}{d\theta}(\lambda_i + \alpha_i) = 0$$

$$\frac{d^2x_i}{d\theta^2}(\lambda_i + \alpha_i) = 0$$

These conditions result in the following values for the constants

$$a_i = 10\frac{(x_{ei} - x_{si})}{\alpha_i^{\,3}}$$

$$b_i = -15\frac{(x_{ei} - x_{si})}{\alpha_i^{\,4}}$$

$$c_i = 6\frac{(x_{ei} - x_{si})}{\alpha_i^{\,5}}$$

A3. The **Cycloidal Curve**

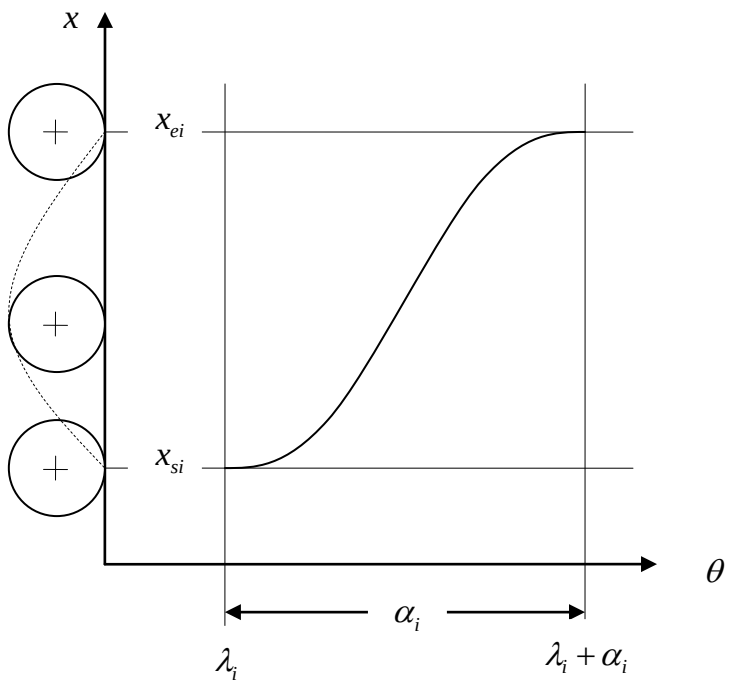

Figure A.3. The Cycloid adopted for Curve Section Number i

The cycloid is a curve traced by a point on the circumference of a circular disk as it rolls without slipping on a flat surface. Based on the definitions given above for the end and final conditions of the curve, the following equation can be written for the cycloidal piston motion;

$$x = x_{si} + \frac{(\theta - \lambda_i)}{\alpha_i}(x_{ei} - x_{si}) - \frac{(x_{ei} - x_{si})}{2\pi} Sin2\pi \frac{(\theta - \lambda_i)}{\alpha_i}$$

---------- E N D ----------